© 2014. Published by The Company of Biologists Ltd | Journal of Cell Science (2014) 127, 5189–5203 doi:10.1242/jcs.150623

RESEARCH ARTICLE

CLIC4 regulates cell adhesion and β1 integrin trafficking

Elisabetta Argenzio‡, Coert Margadant*, Daniela Leyton-Puig, Hans Janssen, Kees Jalink, Arnoud Sonnenberg and Wouter H. Moolenaar‡

ABSTRACT

Chloride intracellular channel protein 4 (CLIC4) exists in both soluble and membrane-associated forms, and is implicated in diverse cellular processes, ranging from ion channel formation to intracellular membrane remodeling. CLIC4 is rapidly recruited to the plasma membrane by lysophosphatidic acid (LPA) and serum, suggesting a possible role for CLIC4 in exocytic–endocytic trafficking. However, the function and subcellular target(s) of CLIC4 remain elusive. Here, we show that in HeLa and MDA-MB-231 cells, CLIC4 knockdown decreases cell–matrix adhesion, cell spreading and integrin signaling, whereas it increases cell motility. LPA stimulates the recruitment of CLIC4 to β1 integrin at the plasma membrane and in Rab35-positive endosomes. CLIC4 is required for both the internalization and the serum- or LPA-induced recycling of β1 integrin, but not for EGF receptor trafficking. Furthermore, we show that CLIC4 suppresses Rab35 activity and antagonizes Rab35-dependent regulation of β1 integrin trafficking. Our results define CLIC4 as a regulator of Rab35 activity and serum- and LPA-dependent integrin trafficking.

KEY WORDS: CLIC4, Cell adhesion, Integrin trafficking, Lysophosphatidic acid, Rab35

INTRODUCTION

The chloride intracellular channel (CLIC) protein family consists of six members (CLIC1–CLIC6) that are structurally related to the omega class of glutathione S-transferases (GSTs), but appear to have distinct cellular functions (Dulhunty et al., 2001; Harrop et al., 2001; Jiang et al., 2014; Littler et al., 2005; Littler et al., 2010). CLICs are globular proteins that are highly conserved among vertebrates and exist in both soluble and membrane-associated forms. They have been implicated in membrane remodeling, intracellular trafficking, vacuole formation, actin reorganization, ion transport and other processes (for a review, see Jiang et al., 2014; Littler et al., 2010).

Gene targeting studies in mice have begun to reveal essential, non-redundant physiological roles of the CLIC proteins, including in platelet and macrophage function (Jiang et al., 2012; Qiu et al., 2010), hearing (Gagnon et al., 2006), angiogenesis and wound healing (Padmakumar et al., 2012; Ulmasov et al., 2009). In *Caenorhabditis elegans*, disruption of the CLIC homolog EXC-4 dramatically impairs formation and maintenance of the intracellular excretory tube, but vertebrate CLICs cannot rescue the phenotype, indicating that vertebrate and invertebrate CLICs have distinct functions (Berry et al., 2003; Berry and Hobert, 2006).

Among the six mammalian CLIC proteins, CLIC4 is the best-studied family member, yet its precise function(s) and regulation are still largely unknown. CLIC4 is ubiquitously expressed and detected in the cytosol as a diffusible protein, but it can also localize to intracellular vesicles, organelles and actin-based structures (Berryman and Goldenring, 2003; Chuang et al., 1999; Chuang et al., 2010) and even to the nucleus (Shukla et al., 2009; Suh et al., 2007). Growing evidence points to a role for CLIC4 in such diverse processes as angiogenesis, differentiation, migration and wound healing. Thus, *Clic4*$^{-/-}$ mice display defective angiogenesis and vacuolization (Ulmasov et al., 2009) as well as spontaneous skin erosions and impaired wound healing, apparently due to defects in cell adhesion (Padmakumar et al., 2012). However, the underlying mechanism is unknown. Cell adhesion is mediated by integrins, heterodimeric transmembrane receptors that link the extracellular matrix to the cytoskeleton. Integrins undergo endocytic–exocytic trafficking, both constitutively and in a stimulus-dependent manner. Integrin endocytic recycling is key to the regulation of cell adhesion, spreading and migration (Bridgewater et al., 2012; Caswell et al., 2009; Margadant et al., 2011; Pellinen and Ivaska, 2006).

We previously identified CLIC4 as a new player in a signaling pathway initiated by G-protein-coupled receptor agonists, in particular the lipid mediator lysophosphatidic acid (LPA) (Ponsioen et al., 2009). LPA is a major serum constituent (Eichholtz et al., 1993) and many cellular responses to serum are in fact attributable to LPA receptor stimulation (Moolenaar et al., 2004). Using N1E-115 neuroblastoma cells as a model, we showed that CLIC4 undergoes rapid but transient translocation from the cytosol to distinct regions of the plasma membrane upon LPA or serum stimulation, in a manner strictly dependent on RhoA activity and F-actin integrity (Ponsioen et al., 2009). This observation raises the possibility that CLIC4 functions in a regulated exocytic–endocytic trafficking route; however, very little is known about the rapid agonist-induced recruitment of CLIC4 to the plasma membrane.

In the present study, we set out to examine the function and LPA-induced redistribution of CLIC4 in HeLa and MDA-MB-231 carcinoma cells, focusing on cell adhesion and integrin behavior. We find that CLIC4 is required for integrin-mediated cell adhesion, and that LPA stimulates the recruitment of CLIC4 to β1 integrin at the plasma membrane and in Rab35-positive endosomes. CLIC4 stimulates both the internalization and serum/LPA-induced recycling of β1 integrin. Furthermore, CLIC4 suppresses Rab35 activity, and antagonizes Rab35-dependent regulation of integrin trafficking. We conclude that CLIC4 is a new player in the agonist-regulated trafficking of β1 integrin.

Division of Cell Biology, The Netherlands Cancer Institute, Plesmanlaan 121, 1066CX Amsterdam, The Netherlands.
*Present address: Department of Molecular Cell Biology, Sanquin Research, Plesmanlaan 125, 1066CX Amsterdam, The Netherlands.

‡Authors for correspondence (e.argenzio@nki.nl; w.moolenaar@nki.nl)

Received 24 January 2014; Accepted 13 October 2014

Journal of Cell Science (2014) 127, 5189–5203 doi:10.1242/jcs.150623

RESULTS

Generation and analysis of CLIC4-knockdown cells

To examine the cellular function(s) of CLIC4, we knocked down CLIC4 expression in HeLa and MDA-MB-231 cells, which are widely used models in epithelial cell adhesion studies. CLIC4-depleted cells were obtained using lentiviral vectors containing different small hairpin RNAs (shRNAs) against CLIC4 (denoted shCLIC4). We raised a CLIC4-specific polyclonal antibody (Fig. 1A), and confirmed stable CLIC4 knockdown by western blotting and quantitative PCR (qPCR). Among five distinct shRNAs tested, shCLIC4(#3) and shCLIC4(#5) were the most effective (Fig. 1B,C; and data not shown). CLIC4 knockdown did not affect the rate of cell proliferation, nor did it modulate EGF- or LPA-induced activation of ERK1/2 (also known as MAPK3 and MAPK1, respectively) and AKT1 (supplementary material Fig. S1), indicating that CLIC4 has no direct role in mitogenic signaling. Furthermore, CLIC4-depleted cells showed RhoA-mediated cytoskeletal contraction and developed stress fibers upon LPA stimulation, similar to control cells, which argues against a role for CLIC4 in actin remodeling (results not shown; see also Ponsioen et al., 2009). When assessing cell morphology and adhesion, however, we observed that CLIC4-depleted cells consistently appeared less well spread (at 24 h after plating) and adhered less efficiently to the plates than did control cells, suggesting a defect in integrin function. We therefore focused our studies on the role of CLIC4 in cell–matrix adhesion and integrin function.

CLIC4 regulates integrin-dependent cell adhesion, motility and focal adhesion assembly

We first determined the level of adhesion of CLIC4-depleted and control cells (containing empty vector) to the integrin-binding substrates collagen-I and fibronectin, at 30 min after plating in serum-free medium. As shown in Fig. 1D, CLIC4-depleted HeLa and MDA-MB-231 cells, containing either shCLIC4(#3) or shCLIC4(#5), adhered less well to these substrates. To rescue this phenotype, HeLa cells containing shCLIC4(#3) were transiently transfected with either an shRNA-resistant mouse version of CLIC4 (GFP–mCLIC4) or mCherry alone (Fig. 1E, left panel), mixed in a 1:1 ratio, and seeded on collagen-coated surfaces. Expression of GFP–mCLIC4 rescued cell adhesion to collagen-I, as quantified by counting the number of red and green cells (Fig. 1E, middle panel). Cell adhesion to fibronectin was similarly rescued (Fig. 1E, right panel).

We next examined how the reduced cell–matrix adhesion of the CLIC4-depleted cells affected cell motility by using time-lapse video microscopy. Under serum-free conditions, CLIC4-depleted MDA-MB-231 cells migrated significantly faster than control cells on collagen-I, consistent with reduced cell adhesion. LPA, an established motility factor, enhanced the random motility of control cells, but not that of CLIC4-depleted cells (Fig. 1F, left panel). LPA did not affect cell directionality in either control or CLIC4-depleted cells (Fig. 1F, right panel). Taken together, these results suggest that CLIC4 depletion leads to maximal cell motility, rendering the cells unresponsive to further stimulation by LPA.

Integrin-ligand binding leads to focal adhesion formation, protein phosphorylation and cell spreading (Geiger and Yamada, 2011). At 1 h after plating on collagen-I or fibronectin in serum-free medium, CLIC4-depleted HeLa cells appeared less spread than control cells (Fig. 2A,B and Fig. 2E,F, respectively). Vinculin staining of spreading cells revealed that shCLIC4 cells had reduced focal adhesion size and number when compared to cells containing control shRNA (denoted shControl), indicative of impaired focal adhesion assembly (Fig. 2A,C,D and Fig. 2E,G,H on collagen-I or fibronectin, respectively). We measured the autophosphorylation of focal adhesion kinase (FAK, also known as PTK2) on residue Y397 (FAK-pY397), a well-established readout of integrin signaling (Parsons, 2003). Upon plating on either collagen-I or fibronectin, HeLa cells showed an increase in FAK-pY397 levels over time, with a maximum reached at ~60 min after seeding. CLIC4-depleted cells showed significantly less FAK-pY397 under similar conditions (Fig. 2I,J), consistent with reduced focal adhesion assembly and cell spreading. From these results, we conclude that CLIC4 is required for the regulation of integrin-mediated events, notably cell–matrix adhesion, cell spreading, focal adhesion assembly and cell motility.

LPA stimulation recruits CLIC4 to β1 integrin

We have previously reported that CLIC4 undergoes rapid but transient translocation from the cytosol to the plasma membrane upon LPA or serum stimulation in various cell types, including N1E-115, A431 and HeLa cells (Ponsioen et al., 2009). Given the apparent role of CLIC4 in integrin-mediated processes, we examined whether CLIC4 is recruited to integrins at the plasma membrane upon LPA stimulation. We focused on the ubiquitously expressed β1 integrin, which mediate adhesion to collagens and fibronectin.

We examined the localization of CLIC4 and the integrin β1 subunit in both serum-starved and LPA-stimulated HeLa cells by super-resolution microscopy, using the ground-state depletion imaging method (Fölling et al., 2008). This technique offers exceptional optical resolution down to ~10 nm, allowing us to obtain dual-color super-resolution images of GFP–CLIC4 and the integrin β1 subunit in total internal reflection fluorescence mode. In serum-starved cells, CLIC4 distribution was mainly cytosolic, whereas β1 integrin was mainly found at the plasma membrane, although some CLIC4–integrin-β1 colocalization was also observed (Fig. 3A). Following stimulation with 1-oleoyl-LPA (1 μM; 2 min), significantly more CLIC4 was detected at the plasma membrane, where it prominently colocalized with β1 integrin; enhanced CLIC4–integrin-β1 colocalization was also detected in intracellular compartments (Fig. 3A,B). Of note, the internal β1 integrin pool that colocalized with CLIC4 was predominantly in the active conformation, as shown by using an antibody that recognizes active β1 integrin only (Fig. 3C).

LPA-induced colocalization of CLIC4 and β1 integrin was confirmed by electron microscopy using gold-labeled ultra-thin sections of LPA-treated MDA-MB-231 cells (Fig. 3D). These results show that LPA stimulation recruits CLIC4 to β1 integrin, both at the plasma membrane and in intracellular compartments.

CLIC4 regulates integrin internalization, and LPA- and serum-induced recycling

To investigate how CLIC4 recruitment to β1 integrin might affect integrin-β1-mediated cell adhesion, we determined integrin expression under steady-state conditions. Through flow cytometry and western blotting, we established that CLIC4 depletion did not affect the cell surface expression of β1 integrin or other β- and α-subunits (Fig. 4A; supplementary material Table S1), nor did it affect the levels of the precursor and mature forms of β1 integrin (Fig. 4B). Thus, the observed effects of CLIC4 silencing on cell adhesion are not simply due to differences in integrin expression.

Journal of Cell Science (2014) 127, 5189–5203 doi:10.1242/jcs.150623

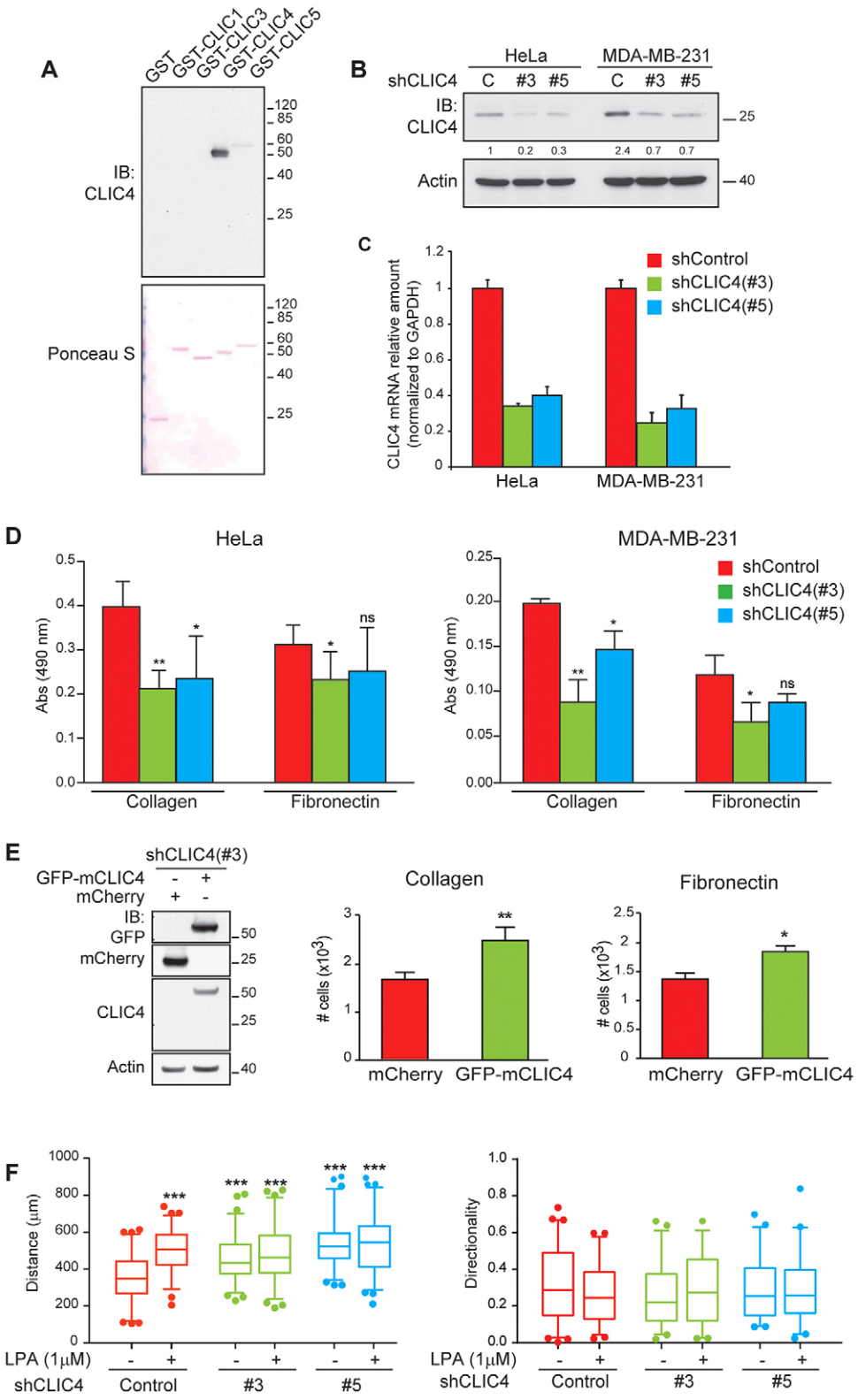

Fig. 1. CLIC4 knockdown affects cell adhesion and motility. (A) Immunoblot (IB) showing the antibody specificity for CLIC4. Distinct CLICs were purified as GST fusion proteins. Ponceau-S staining shows equal protein loading. (B,C) CLIC4 knockdown in HeLa and MDA-MB-231 cells. For stable knockdown, cells were infected with lentiviral particles as described in the Materials and Methods. Two distinct shRNAs targeting CLIC4 are shown. The control population was obtained using empty vector (labeled C in panel B). (B) Knockdown efficiency determined by immunoblotting of total cell lysate using anti-CLIC4 antibody; β-actin was used as loading control. The relative amount of CLIC4 determined by densitometry (ImageJ software) is indicated, using the HeLa cell control lane as reference. (C) CLIC4 mRNA levels (normalized to GAPDH) were determined by qPCR. (D) Cell–matrix adhesion assays. shControl and shCLIC4 cells were plated on collagen-I or fibronectin. At 30 min after plating, non-adherent cells were washed away and adherent cells were fixed. For quantification, cells were stained with Crystal Violet. The plots represent the mean±s.d. of three independent experiments. (E) Rescue of the CLIC4-deficient phenotype. Left panel: shCLIC4 cells were transfected with mCherry or the mouse version of GFP–CLIC4 (mCLIC4). Expression of mCherry and GFP–mCLIC4 was detected by immunoblot analysis using antibodies against GFP, RFP and CLIC4; β-actin was used as loading control. Middle and right panels: cells were mixed in 1:1 ratio and seeded on collagen and fibronectin, and treated as in A. The number of red- and green-stained cells was counted using the ImageJ software. The plots represent mean±s.d. of two independent experiments. (F) CLIC4 and random cell motility. MDA-MB-231 cells were plated on collagen and allowed to adhere for 48 h. Cells were serum starved overnight and stimulated with 1 μM LPA or left untreated prior to time-lapse imaging. Images were captured every 2 min during 8 h, and the distance covered by the cells and the directionality were analyzed using ImageJ software. Data represent the distance (left panel) and directionality (right panel) in three independent experiments (n=62 cells). The box represents the 25th to 75th percentiles, and the median is indicated by the line, the whiskers represent the 5th–95th percentiles. *P<0.05, **P<0.01, ***P<0.001; ns, not significant.

Aside from integrin expression, the dynamic regulation of integrin internalization and recycling plays a key role in cell adhesion and motility (Arjonen et al., 2012; Caswell and Norman, 2006; Margadant et al., 2011; Roberts et al., 2001). Integrin recycling is controlled by serum and LPA (White et al., 2007), and LPA stimulation recruits CLIC4 to integrins both at the plasma membrane and in intracellular compartments (Fig. 3). We therefore examined whether depletion of CLIC4 might affect the trafficking of β1 integrin, using confocal microscopy, biochemical assays and flow cytometry. We first employed an antibody-based assay, in which shControl and shCLIC4 HeLa and MDA-MB-231 were incubated with anti-β1-integrin antibody (TS2/16) at 4℃. Thereafter, internalization of cell surface β1 integrin was initiated by transfer to serum-free medium at 37℃

Journal of Cell Science (2014) 127, 5189–5203 doi:10.1242/jcs.150623

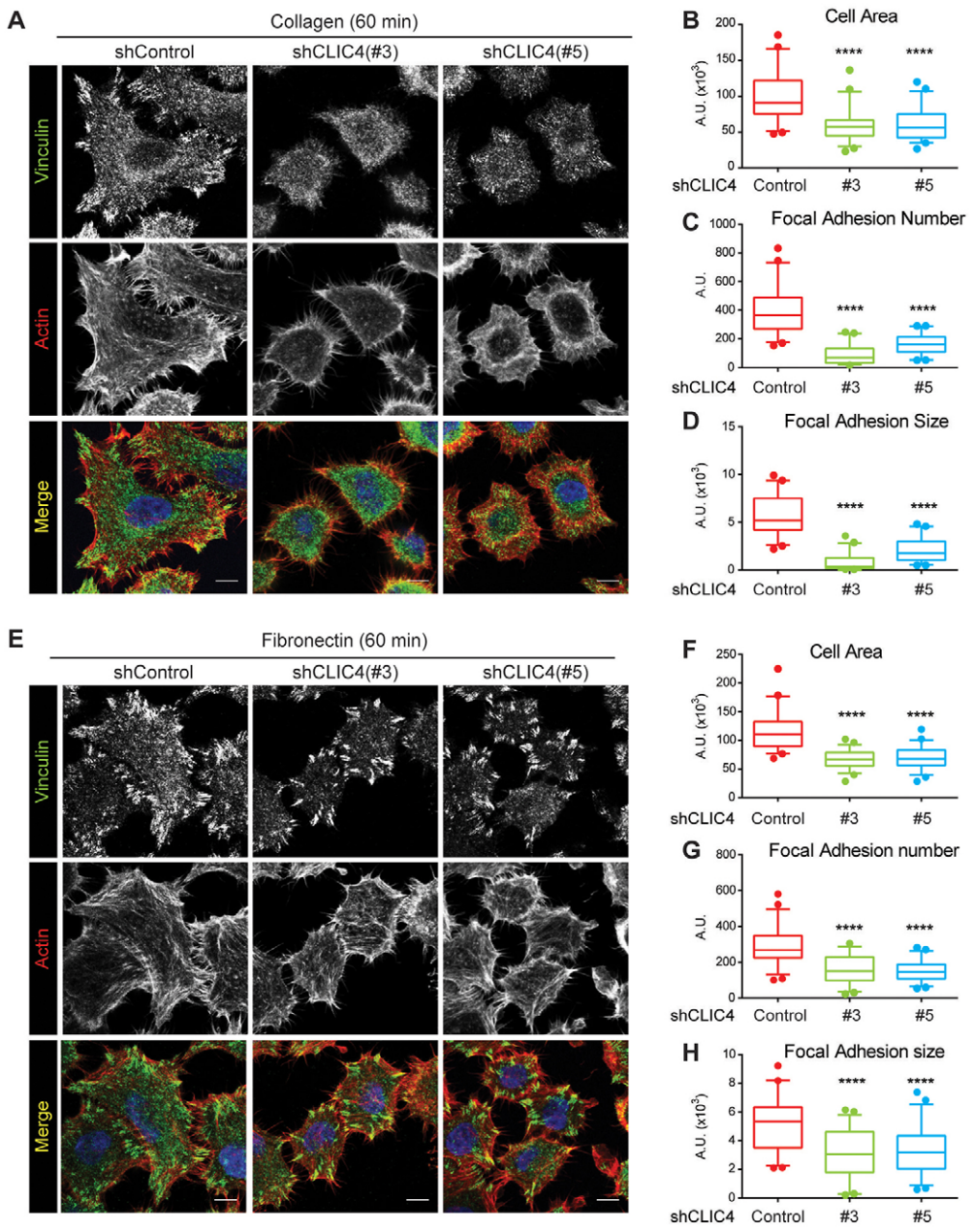

Fig. 2. CLIC4 depletion reduces cell spreading, focal adhesion assembly and integrin signaling. shControl and shCLIC4 HeLa cells were seeded on collagen-I- (A–D) or fibronectin-coated coverslips (E–H) for 60 min. Adherent cells were fixed with PFA. Confocal sections of cells stained with phalloidin (red), vinculin (green) and DAPI (blue) cells are shown. Scale bars: 10 μm. Plots represent the quantification of cell area (B,F), focal adhesion number (C,G) and focal adhesion number (D,H) using ImageJ software (two independent experiments; $n=50$ cells). The box represents the 25th to 75th percentiles, the median is indicated by the line, the whiskers represent the 5th–95th percentiles. ****$P<0.0001$.
(I,J) Integrin signaling, as measured by FAK activity. shControl and shCLIC4 HeLa cells were seeded on collagen (I) or fibronectin (J) for the indicated time. Activation of FAK was analyzed by immunoblotting using anti-FAK-pY397 antibody. Anti-FAK and β-actin immunoblots were used as loading control. Representative blots of one out of three independent experiments are shown. Densitometric analysis (mean±s.e.m) of three experiments is shown under the blots. ****$P<0.0001$.

Journal of Cell Science (2014) 127, 5189–5203 doi:10.1242/jcs.150623

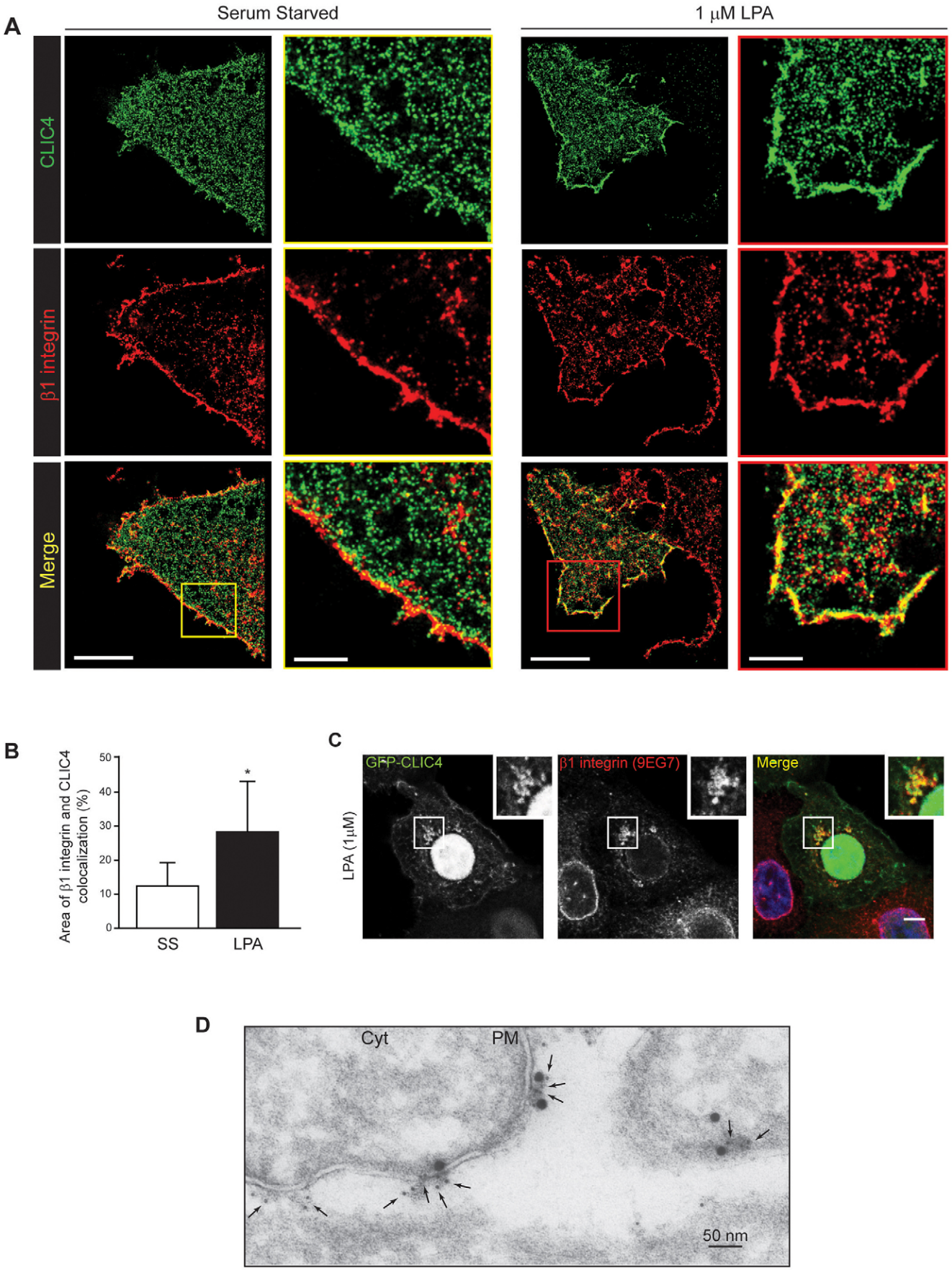

Fig. 3. See next page for legend.

Journal of Cell Science (2014) 127, 5189–5203 doi:10.1242/jcs.150623

Fig. 3. LPA induces colocalization of CLIC4 with β1 integrin. (A) HeLa cells on collagen-coated coverslips were transfected with GFP–CLIC4. Dual-color super-resolution images show CLIC4 (green) and β1 integrin (red). Cells were stimulated with 1 μM LPA for 2 min or left untreated. Scale bar: 5 μm. Boxed areas are shown at higher magnification on the right. Scale bar: 1.5 μm. (B) Colocalization between CLIC4 and β1 integrin was measured as the CLIC4-positive area inside the β1-integrin-positive area (100%) at the plasma membrane. The plot represents mean±s.e.m. of three independent experiments ($n=7$ cells). *$P<0.05$. (C) CLIC4 colocalizes with active β1 integrin upon LPA stimulation. HeLa cells were seeded on collagen-coated coverslips, transfected with GFP–CLIC4, serum starved overnight and stimulated with LPA for 2 min. Confocal images show GFP–CLIC4 (green), active β1 integrin (antibody 9EG7, red) and DAPI (blue). (D) Immunoelectron microscopy of LPA-stimulated MDA-MB-231 cells. Cells on collagen-I-coated dishes were stimulated with 1 μM LPA for 2 min, and fixed cells were collected for ultrathin sectioning. CLIC4 and β1 integrin were stained with large and small gold particles, respectively. Arrows point to β1 integrin. Cyt, cytoplasm; PM, plasma membrane.

(Arjonen et al., 2012; Margadant et al., 2013; Powelka et al., 2004). Recycling of internalized β1 integrin was then induced by stimulation with serum. As shown in Fig. 5A,B), rapid recycling (within 5 to 15 min) of internalized β1 integrin back to the plasma membrane occurred in control cells. In marked contrast, redistribution of the internal integrin pool to the plasma membrane was strongly reduced in CLIC4-depleted cells, as quantified in Fig. 5C. Similar results were obtained using LPA alone (data not shown). It thus appears that CLIC4 is important for the serum- and LPA-regulated, synchronized recycling of internalized β1 integrin.

To quantify this process, we measured integrin trafficking using a biotin-labeling and enzyme-linked immunosorbent assay (ELISA) protocol, focusing on integrin α5β1 (Roberts et al., 2001) (see Materials and Methods). Consistent with the above results, 55% of the internalized integrin α5β1 had already recycled back to the plasma membrane in control cells after 5 min of serum stimulation, whereas only 19% had recycled in CLIC4-depleted cells (Fig. 6A). Recycling in the absence of CLIC4 was also reduced at later time points. In addition, reduced recycling of β1 integrin in general was confirmed in a FACS-based assay, using an anti-β1 antibody and two distinct shRNAs against CLIC4 (supplementary material Fig. S2A).

We also examined whether CLIC4 was required for integrin endocytosis by measuring the internalization of integrin α5β1, using the aforementioned biotin-labeling protocol followed by capture ELISA. We found that the pool of internalized integrin α5β1 (under serum-free conditions), as induced by a temperature shift from 4℃ to 37℃, was reduced by ∼50% in CLIC4-depleted cells (Fig. 6B; supplementary material Fig. S2B). Integrin internalization and subsequent sorting in the endosomal system determine the amount of integrin that is returned to the plasma membrane. It has recently become clear that β1 integrin, in particular integrin α5β1, is sorted to late endosomes and lysosomes, much like growth factor receptors, and that the balance between recycling and internalization depends on sorting signals in the cytoplasmic tail of β1 and ubiquitylation (Böttcher et al., 2012; Dozynkiewicz et al., 2012; Lobert et al., 2010; Margadant et al., 2012; Steinberg et al., 2012). We therefore investigated whether the recycling defect in CLIC4-knockdown cells led to increased degradation. Cell surface integrins were biotinylated, and subsequently the cells were incubated in complete medium to allow for internalization and recycling (up to 6 h). Comparable to the turnover observed in other cell systems, more than 50% of α5β1 was degraded within 6 h. Similar kinetics of integrin degradation were observed in the CLIC4-depleted cells (Fig. 6C).

Taken together, these results show that CLIC4 regulates both the constitutive endocytosis and the serum- and LPA-regulated recycling of β1 integrin, without affecting integrin degradation.

CLIC4 is not required for EGFR trafficking

We next asked whether the effect of CLIC4 on integrin trafficking is specific. We focused on the EGF receptor (EGFR), which has been shown to co-traffic with integrin α5β1 (Caswell et al., 2008; Muller et al., 2009). As shown in Fig. 6D, CLIC4 depletion did not alter the steady-state levels of EGFR at the plasma membrane in

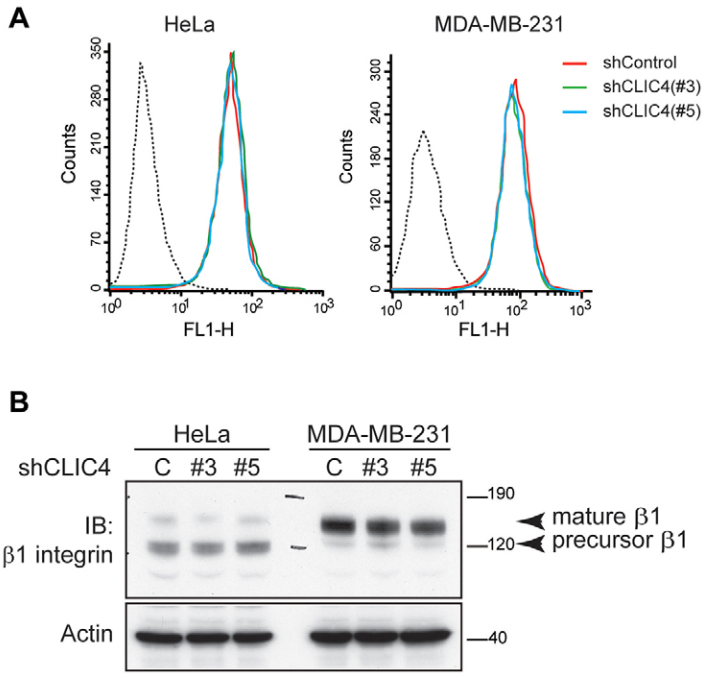

Fig. 4. CLIC4 knockdown does not affect β1 integrin expression. (A) shControl and shCLIC4 HeLa and MDA-MB-231 cells were trypsinized, incubated with anti-β1-integrin antibody and analyzed by flow cytometry. Staining with secondary antibody only was used as a negative control (dashed black line). Representative histograms of one out of three independent experiments indicate that CLIC4 knockdown does not affect the surface levels of β1 integrin. (B) Expression of precursor and mature β1 integrin in shControl and shCLIC4 cells was analyzed by immunoblot (IB) analysis of total cell lysates. β-actin was used as loading control.

Journal of Cell Science (2014) 127, 5189–5203 doi:10.1242/jcs.150623

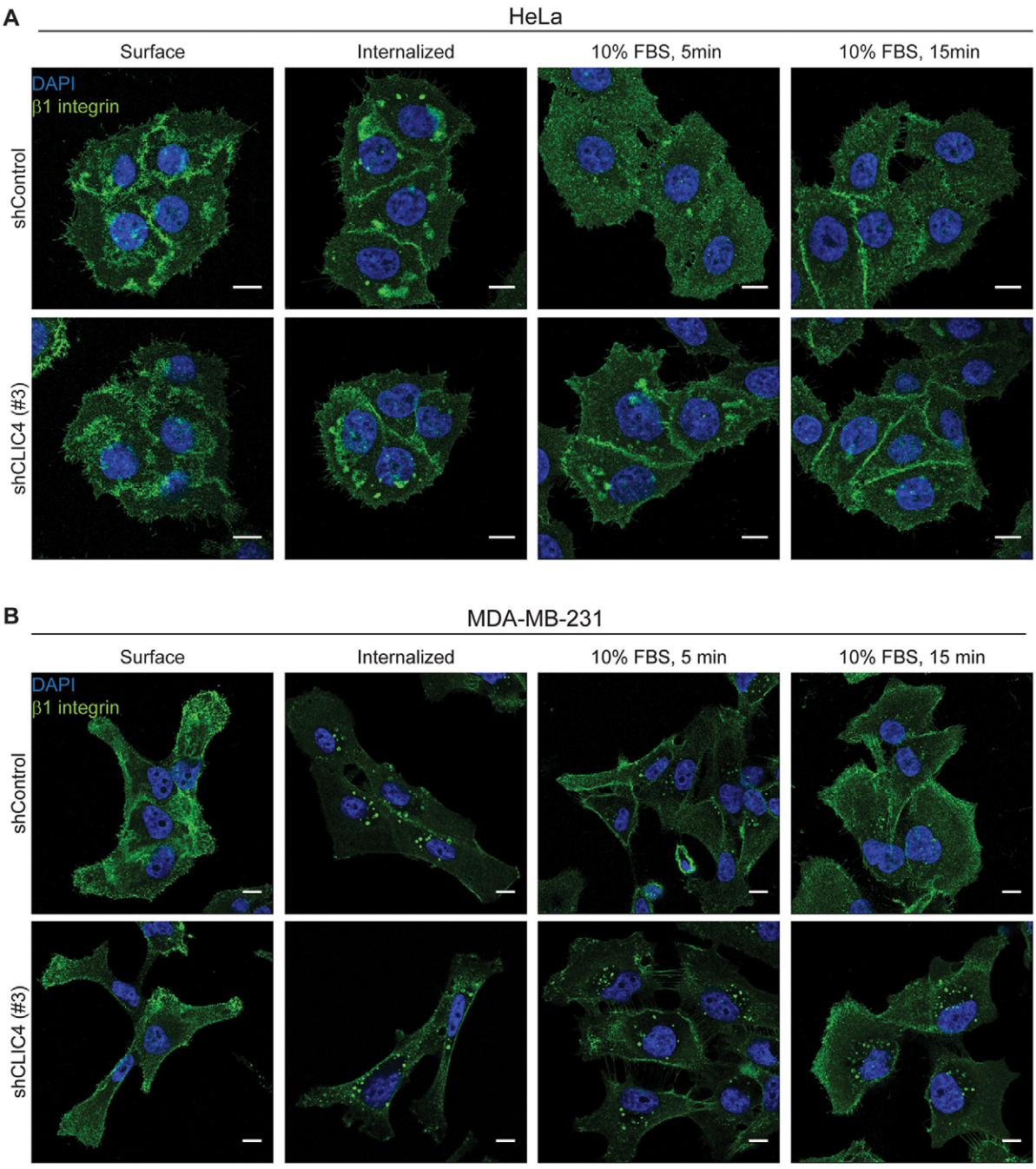

C

	cells with recycled integrin (%)			
	HeLa		MDA-MB-231	
	5 min	*15 min*	*5 min*	*15 min*
shControl	71	100	55	80
shCLIC4	17	45	19	56

Fig. 5. CLIC4 regulates serum-stimulated integrin recycling. (A,B) Antibody-based integrin recycling assay. shControl and shCLIC4#3 HeLa (A) and MDA-MB-231 (B) cells on collagen-coated coverslips were serum starved and labeled with anti-β1-integrin antibody TS2/16. β1 integrin internalization was allowed for 2 h at 37°C in serum-free medium. Integrin recycling was stimulated by 10% FBS for the indicated time periods. Images represent confocal sections of β1 integrin (green) and DAPI-stained (blue) cells. Scale bars: 10 μm. (C) The percentage of cells with recycled β1 integrin at 5 and 15 min from two independent experiments is indicated (n=17–26).

Journal of Cell Science (2014) 127, 5189–5203 doi:10.1242/jcs.150623

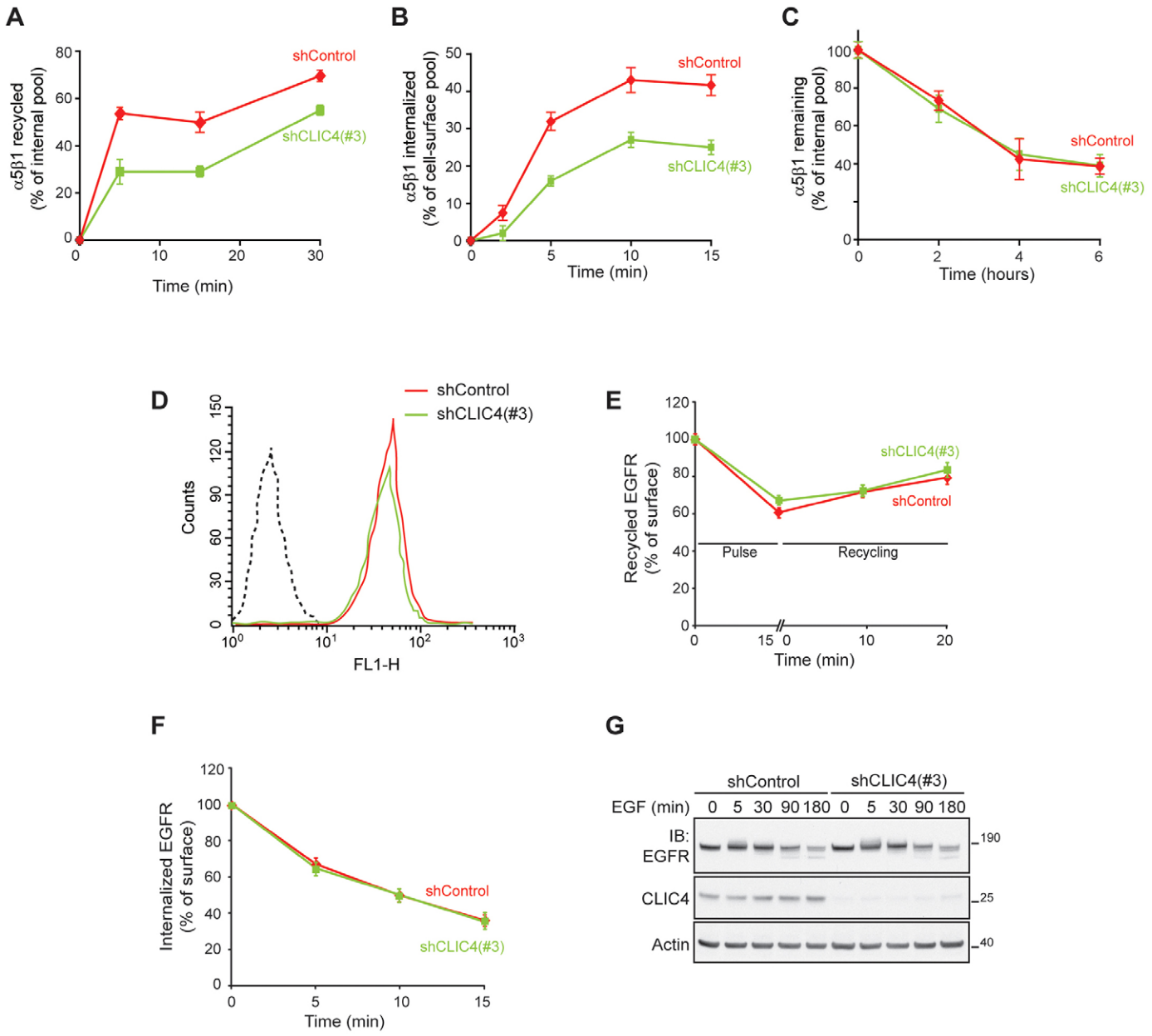

Fig. 6. CLIC4 regulates the internalization and recycling of integrin α5β1, but not of EGFR. (A) CLIC4 knockdown reduces integrin recycling. shControl and shCLIC4 HeLa cells were surface-labeled with NHS-S-S-Biotin. Internalization was allowed to proceed for 30 min at 37˚C. Cell surface biotin was reduced with MesNa at 4˚C, and the cells were incubated with 10% FBS at 37˚C for the indicated time periods to promote recycling of the internal pool. The amount of internalized, biotin-labeled integrins was determined by capture ELISA using a monoclonal antibody against the α5 integrin subunit. (B) CLIC4 knockdown reduces integrin internalization. Cells were biotin-labelled as in A. Following internalization for the indicated times at 37˚C (serum-free conditions), membrane-associated biotin was reduced at 4˚C. The amount of internalized α5β1 integrin was determined as in A. Data in A,B represent mean±s.e.m. of three independent experiments. (C) CLIC4 knockdown does not affect integrin degradation. Biotin-labeled HeLa cells were incubated at 37˚C for the indicated time periods in DMEM plus 10% FBS. The amount of remaining α5β1 integrin was determined as in A,B). Data represent mean±s.e.m. of two independent experiments. (D) CLIC4 knockdown does not affect EGFR cell surface levels. Cells were trypsinized, incubated with anti-EGFR antibody and analyzed by flow cytometry. Staining with secondary antibody only was used as negative control (dashed black line). Representative results from one out of two independent experiments are shown. (E) CLIC4 knockdown does not affect EGFR recycling. Cells were incubated with 20 ng/ml EGF for 1 h on ice, and then shifted at 37˚C for 15 min (pulse) to allow EGFR internalization. Cells were analyzed by flow cytometry. For details see Materials and Methods. The plot represents mean±s.e.m. of two independent experiments. In each assay, 50,000 cells were analyzed for each time point. (F) CLIC4 knockdown does not affect EGFR endocytosis. Cells were labeled with anti-EGFR antibody as in E and subsequently shifted to 37˚C for the indicated time point of internalization. Cells were analyzed by flow cytometry as in E. The plot represents means±s.e.m. of two independent experiments. In each assay, 20,000 cells were analyzed for each time point. (G) CLIC4 knockdown does not affect EGFR degradation. Cells were left untreated or stimulated with 100 ng/ml EGF at 37˚C for the indicated time points. EGFR levels were determined by immunoblot (IB) analysis of total cell lysates using anti-EGFR antibody. β-actin was used as loading control. Representative blots from one out of two experiments are shown.

Journal of Cell Science (2014) 127, 5189–5203 doi:10.1242/jcs.150623

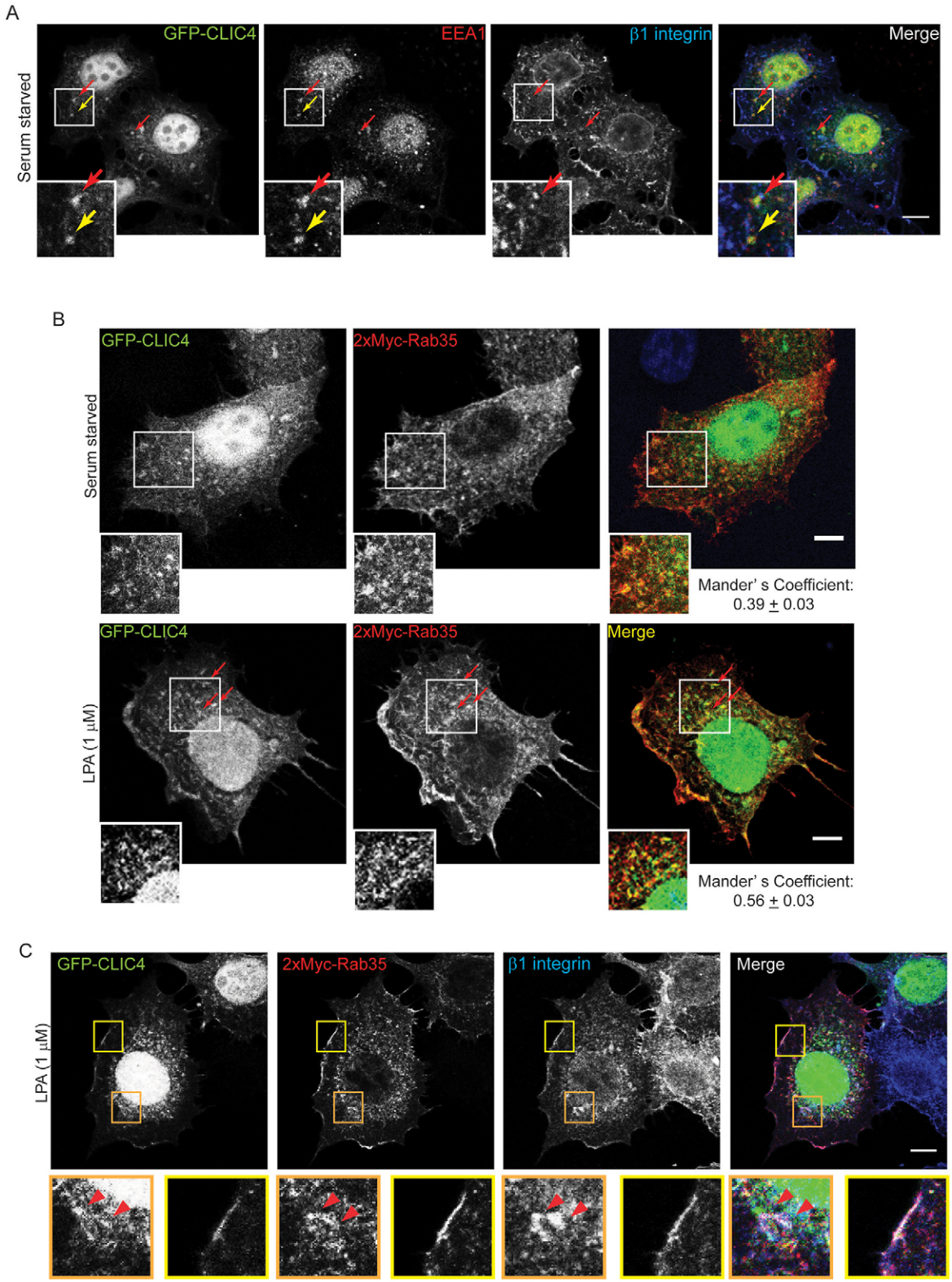

Fig. 7. LPA stimulation directs CLIC4 to Rab35-positive endosomes. HeLa cells on collagen-I-coated coverslips were transfected with the indicated plasmids and serum starved overnight. Cells were then stimulated with LPA for 2 min or left untreated. (A) Confocal images show GFP–CLIC4 (green), EEA1 (red) and β1 integrin (blue). Red arrows, compartments positive for CLIC4, EEA1 and β1 integrin. Yellow arrows, compartments positive for CLIC4 and EEA1. (B) Confocal images show GFP–CLIC4 (green), 2×Myc–Rab35 (red) and DAPI (blue). Arrows indicate compartments positive for CLIC4 and Rab35. Where indicated, LPA was added for 2 min. Red arrows indicate compartments positive for CLIC4 and Rab35. The Mander's coefficient (mean±s.e.m.) was calculated using the ImageJ software (n=25 cells, from three independent experiments, P<0.0005 between the two conditions). (C) Confocal images show GFP–CLIC4 (green), 2×Myc–Rab35 (red) and β1 integrin (blue) in LPA-stimulated cells. Arrowheads point to tripartite colocalization of CLIC4, Rab35 and β1 integrin at the plasma membrane (yellow box) and in internal compartments (orange box). Boxed areas in A–C are shown at higher magnification. Scale bars: 10 μm.

Journal of Cell Science (2014) 127, 5189–5203 doi:10.1242/jcs.150623

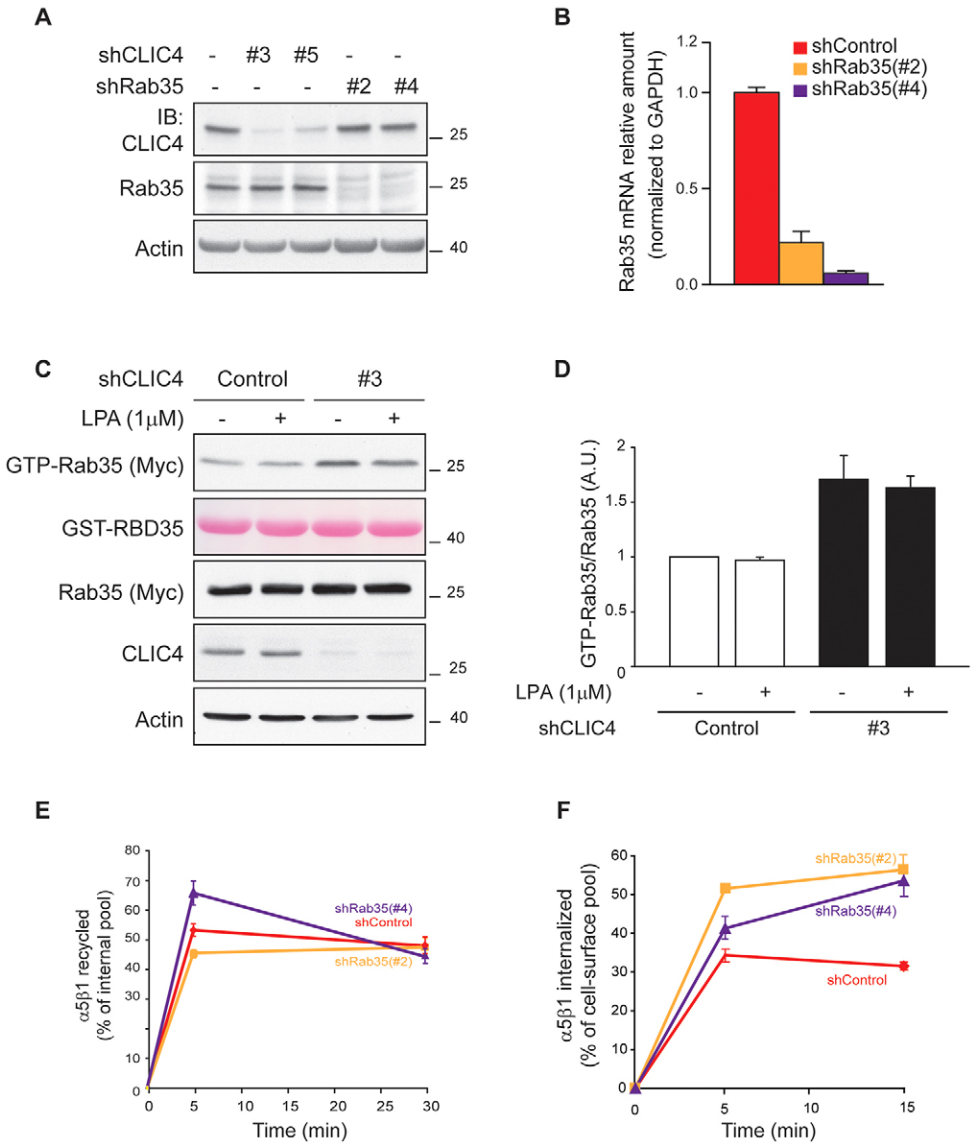

Fig. 8. CLIC4 suppresses Rab35 activity and has opposing effects on Rab35-regulated integrin trafficking. (A,B) Rab35 knockdown in HeLa cells. Stable Rab35 knockdown cells were obtained as described in the Materials and Methods. Two distinct shRNAs targeting Rab35 are shown. Control cells were obtained using empty vector. In A, knockdown efficiency was determined by immunoblotting (IB) using anti-Rab35 antibody; β-actin was used as loading control. In B, Rab35 mRNA levels (normalized to GAPDH) were determined by qPCR. (C,D) CLIC4 knockdown stimulates Rab35 activation in an LPA-independent manner. GTP-Rab35 pull-down assay. shControl and shCLIC4 cells were transfected with 2×Myc–Rab35, serum starved overnight and left untreated or stimulated with 1 μM LPA for 2 min. GST–RBD35 was incubated with total cell lysates from transfected cells. GTP-Rab35 bound to the beads was analyzed by immunoblot analysis. Total Rab35 was determined by immunoblot analysis of total cell lysate (5%). Ponceau-S staining shows equal GST–RBD35 loading. Representative blots of one out of three experiments are shown. D shows densitometric analysis of three independent experiments (mean±s.d.). (E) Rab35 knockdown does not affect integrin recycling. Cells were biotin-labeled and treated as described in Fig. 7A. Data represent mean±s.e.m. of two independent experiments. (F) Rab35 knockdown increases integrin endocytosis. shControl and shRab35 HeLa cells were surface-labeled with NHS-S-S-Biotin and treated as described in Fig. 7B. Data represent means±s.e.m. of two independent experiments.

HeLa cells. Furthermore, CLIC4 silencing did not affect ligand-induced EGFR recycling, nor did it affect EGFR endocytosis, as measured by flow cytometry (Sigismund et al., 2008) (Fig. 6E,F). After EGF stimulation, EGFR levels decreased over time, indicative of degradation, in a manner independent of CLIC4 (Fig. 6G). It thus appears that CLIC4 is not required for ligand-induced trafficking and degradation of EGFR. On the basis of these results, we conclude that CLIC4 regulates the trafficking of β1 integrin in a specific manner.

CLIC4 colocalizes with β1 integrin in early and Rab35-positive endosomes

Small GTPases of the Rab family are key regulators of membrane trafficking and define distinct populations of early, late and recycling endosomes. To identify the trafficking compartments where CLIC4 might meet β1 integrin, we used several Rab GTPases as endosomal markers, as well as the Rab-5 effector early endosome antigen 1 (EEA-1), a marker of early endosomes, and lysosomal-associated membrane protein 1 (LAMP1), a marker for late endosomes and lysosomes. In GFP–CLIC4-expressing HeLa cells, CLIC4 did not colocalize with Arf6, Rab4a, Rab7, Rab11A or LAMP1, neither in serum-starved nor in serum-stimulated cells (data not shown). However, a small subpopulation of CLIC4 was found to colocalize with β1 integrin in EEA1-positive early endosomes, consistent with the observed effect of CLIC4 on integrin endocytosis (Fig. 7A).

We next examined Rab35, which has recently emerged as a regulator of endocytic recycling (Allaire et al., 2010; Allaire et al., 2013; Chua et al., 2010; Kouranti et al., 2006). In serum-starved HeLa cells, Rab35 was mostly found at the plasma membrane and, to a lesser extent, in intracellular compartments (Fig. 7B). Some colocalization of CLIC4 and Rab35 was observed in non-stimulated cells. Upon LPA stimulation for 2 min, CLIC4 showed increased colocalization with Rab35 at the plasma membrane and in intracellular compartments that also contained β1 integrin (Fig. 7C). We conclude that LPA signaling promotes the recruitment of CLIC4 to β1 integrin in Rab35-positive compartments close to the plasma membrane.

CLIC4 affects Rab35 activity

To investigate the relationship between CLIC4 and Rab35 activity in β1 integrin trafficking and LPA signaling, we

Journal of Cell Science (2014) 127, 5189–5203 doi:10.1242/jcs.150623

generated Rab35-depleted HeLa cell lines using two distinct shRNAs. Immunoblot and qPCR analyses showed that Rab35 knockdown did not affect CLIC4 expression, and vice versa (Fig. 8A,B). Furthermore, Rab35 depletion (or expression of a dominant-negative Rab35 mutant) did not affect the ability of LPA to recruit CLIC4 to the plasma membrane, whereas CLIC4 depletion did not detectably alter the subcellular localization of Rab35 (data not shown). Next, we measured the levels of active Rab35-GTP in shControl and CLIC4-depleted HeLa cells before and after LPA stimulation (1 μM; 2 min) by using Rab35-GTP pulldown assays (Fukuda et al., 2011). Interestingly, we observed a twofold increase in Rab35-GTP in CLIC4-depleted cells compared to control cells, both in the absence and presence of LPA (Fig. 8C,D). It thus appears that CLIC4 suppresses Rab35 activity, in a manner independent of LPA signaling.

Opposing effects of CLIC4 and Rab35 on β1 integrin trafficking

We next examined how the observed interplay between CLIC4 and Rab35 affected β1 integrin trafficking using the biotin-labeling and ELISA protocol and flow cytometry in Rab35-depleted versus control cells. Unlike CLIC4, Rab35 was not required for the serum- or LPA-induced recycling of integrin α5β1 (Fig. 8E; data not shown). Furthermore, Rab35 depletion did not affect β1 integrin degradation (data not shown). In marked contrast, the internalization of integrin α5β1 was increased by ~50% upon Rab35 knockdown (Fig. 8F), strongly suggesting that Rab35 is a suppressor of α5β1 internalization. In conclusion, our results indicate that CLIC4, but not Rab35, regulates serum- and LPA-stimulated integrin recycling, whereas CLIC4 and Rab35 have opposing effects on integrin internalization.

DISCUSSION

The present study uncovers a new role for CLIC4 in the serum- and LPA-stimulated recycling of β1 integrin, and underscores the importance of CLIC4 in epithelial cell–matrix adhesion and motility. Building on our previous finding that CLIC4 is rapidly recruited to the plasma membrane in response to LPA (Ponsioen et al., 2009), we now show that LPA stimulation promotes the colocalization of CLIC4 with β1 integrin at the plasma membrane and in Rab35-positive endosomes. CLIC4 appears to be required for both the constitutive internalization of integrin α5β1 as well as its serum- or LPA-dependent recycling. These findings might explain the observed differences in cell–matrix adhesion, focal adhesion assembly, and cell motility upon CLIC4 depletion. Although we find that CLIC4 opposes Rab35 activation and thereby promotes integrin endocytosis (discussed below), it remains to be examined whether CLIC4-regulated cell adhesion and motility requires Rab35. Our results are in line with previous studies, showing that CLIC4 depletion leads to reduced cell adhesion and increased motility in retinal pigment epithelial cells (Chuang et al., 2010), and to reduced cell adhesion in skin keratinocytes (Padmakumar et al., 2012). In the latter study, CLIC4-deficient keratinocytes were found to adhere less efficiently to a matrix secreted by wild-type keratinocytes, and this adhesion defect most likely underlies the impaired wound healing observed in *Clic4*$^{-/-}$ mice (Padmakumar et al., 2012).

Integrin trafficking through the endosomal system has emerged as a pivotal mechanism to regulate integrin function, and requires the concerted action of diverse protein families including kinases, sorting nexins and small GTPases of the Arf and Rab families (Caswell et al., 2009; Margadant et al., 2011; Pellinen and Ivaska, 2006; Rainero and Norman, 2013). Our data now identify CLIC4 as a new player in integrin trafficking, which intriguingly impacts on both internalization and stimulated recycling of β1 integrin. It seems that CLIC4 predominantly colocalizes with internalized integrins in their active conformation, in agreement with the notion that internal integrins consist mainly in their active conformation (Arjonen et al., 2012; Dozynkiewicz et al., 2012; Lobert et al., 2010; Margadant et al., 2012). Given that integrins can co-traffic with growth factor receptors, most notably EGFR, we also tested whether CLIC4 affects EGFR trafficking. Importantly, EGFR endocytosis, recycling and degradation were not affected by CLIC4 depletion, suggesting that CLIC4 acts on specific cargo rather than on vesicular trafficking in general.

Another member of the CLIC family, CLIC3, has been reported to colocalize with integrin α5β1 in late endosomes and lysosomes, and to protect integrin α5β1 from degradation by promoting its recycling to the plasma membrane (Dozynkiewicz et al., 2012). Unlike CLIC3, however, CLIC4 is not detected in late endosomal or lysosomal compartments, and CLIC4 depletion does not affect integrin degradation. This strongly suggests that CLIC4 is not required for the sorting of internalized integrins between recycling and degradation pathways, and also explains the observation that steady-state integrin levels are not reduced in the absence of CLIC4. Thus, CLIC4 and CLIC3 act in distinct subcellular compartments and differentially regulate the fate of internalized β1 integrin. CLIC4 depletion did not affect the levels of other CLIC proteins (data not shown), suggesting that the other family members do not exert compensatory effects.

Consistent with CLIC4 regulating integrin internalization, CLIC4 colocalized with β1 integrin in EEA-1-positive early endosomes. However, CLIC4 did not colocalize with Rab4, a mediator of fast short-loop integrin recycling, or with Rab11, which stimulates long-loop integrin recycling through the perinuclear recycling compartment (Roberts et al., 2001). Instead, CLIC4 colocalized with β1 integrin in a subset of Rab35-positive endosomes. The observation that CLIC4 localizes with β1 integrin in just a subset of all EEA1- or Rab35-positive endosomes suggests that the CLIC4–integrin-β1 interaction is likely to be a short-lived phenomenon, occurring at distinct steps along the integrin trafficking pathway.

Rab35 regulates endocytic trafficking of diverse proteins, and depending on the cargo and cell system, its effects can be either stimulatory or inhibitory (Allaire et al., 2010; Allaire et al., 2013; Chesneau et al., 2012; Kouranti et al., 2006). We find that Rab35 does not affect integrin recycling triggered by LPA or serum, consistent with the observation that Rab35 activity is not detectably altered upon LPA stimulation. Instead, Rab35 suppresses integrin internalization, and CLIC4 and Rab35 thus exert opposing effects on β1 endocytosis. The unexpected finding that Rab35 activity is higher in CLIC4-depleted cells suggests that CLIC4 can stimulate integrin endocytosis through inhibition of Rab35. Possibly, the recruitment of CLIC4 to Rab35-positive compartments is a regulatory mechanism to fine-tune integrin endocytosis. In agreement with our results, a previous study also found no effect of Rab35 on β1 integrin recycling (Allaire et al., 2010). In a subsequent study, however, the authors reported that Rab35 knockdown increased β1 integrin recycling (Allaire et al., 2013). Importantly, in the latter study, cells were incubated for 2 h at 37°C with anti-integrin antibodies, after which surface-bound antibodies were stripped and the appearance on the cell surface of previously internalized integrin–antibody complexes was measured. As such, this set-up does not exclude the

Journal of Cell Science (2014) 127, 5189–5203 doi:10.1242/jcs.150623

possibility that the enhanced 're-surfacing' in the absence of Rab35 is actually the result of increased internalization, consistent with what we find here.

Future studies should address the mechanistic basis of the apparently opposing effects of CLIC4 and Rab35 on β1 integrin endocytosis and how CLIC4 suppresses Rab35 activity. Furthermore, a possible role of Rab35 in CLIC4-mediated cell adhesion remains to be established. One difficulty with such studies is that (1) the precise function of CLIC4 remains elusive, and (2) Rab35 acts on at least six distinct effectors, consistent with Rab35 mediating numerous processes, and that its activity is regulated by multiple guanine-nucleotide-exchange factors and GTPase-activating proteins (Chaineau et al., 2013; Chua et al., 2010).

Elucidating the mode of action of CLIC4 and its family members remains a major challenge. Identification of specific binding partners should help to clarify how CLIC4 acts in integrin trafficking and receptor signaling. In a proteomic screen, we found β1 integrin in GFP–CLIC4 immunoprecipitates, but we were unable to detect a direct interaction (data not shown). Candidate binding partners for CLIC4 include cytoskeletal components (Berryman and Goldenring, 2003; Suginta et al., 2001), but there is as yet no compelling evidence for a strong direct binding between CLIC4 and other proteins. Therefore, CLIC4 interactions are likely to be weak and/or highly dynamic. Such weak and/or transient interactions might allow CLIC4 to briefly interact with distinct partners along a given pathway, thus facilitating signal integration (Jiang et al., 2014),

Of interest, emerging evidence suggests a role for CLIC proteins in intravesicular pH regulation. In endothelial cells, CLIC4 supports intravesicular acidification and vacuolar fusion through an unknown mechanism (Ulmasov et al., 2009). Similarly, CLIC1 contributes to phagosome acidification in macrophages but, again, the underlying mechanism is unknown (Jiang et al., 2012). Vesicular acidification normally is regulated by the V-ATPase-driven proton pump in conjunction with Cl^- channels and Cl^-/H^+ exchangers of the ClC family (unrelated to the CLICs) (Stauber and Jentsch, 2013). Given that Cl^--dependent intravesicular acidification is key to endocytic–exocytic trafficking events, it will be interesting to explore whether CLIC4 (and other CLICs) might modulate, either directly or indirectly, V-ATPase activity or ClC channel function in distinct endocytic compartments.

MATERIALS AND METHODS

Reagents

1-oleyl-LPA, puromycin, fibronectin, MesNa and iodoacetamide were from Sigma. EGF and phalloidin-red (acti-stain™ 555 phalloidin from Cytoskeleton, Inc.) were from Invitrogen. Type-I collagen was from Inamed BioMaterials. EDTA-free protease inhibitor cocktail tablets were from Roche. NHS-SS-Biotin was from Pierce. Antibodies used were: monoclonal anti-β-actin (clone AC-15, Sigma), monoclonal anti-α5 integrin (BD Pharmingen), monoclonal anti-human β1 integrin (clone TS2/16; Developmental Studies Hybridoma Bank and clone 9GE7, a kind gift from Dietmar Vestweber), monoclonal anti-Myc (clone 9E10, Covance), polyclonal anti-CLIC4 (made in-house, see below), polyclonal anti-FAK-pY397 and monoclonal anti-FAK (Cell Signaling), monoclonal anti-vinculin (a gift from Marina Glukhova), anti-EGFR (monoclonal, clone Ab-1, Calbiochem, and polyclonal, clone 1005, Santa Cruz Biotechnology), polyclonal anti-Rab35 (ProteinTech Group, Chicago, IL) and Alexa-Fluor-conjugated secondary antibodies (Invitrogen).

CLIC4 antibody generation

His-tagged CLIC4 was expressed in BL21 *E. coli* and CLIC4 protein was purified using Ni-chromatography and gel filtration. His-tag was removed with TEV protease before rabbit immunization. To obtain a specific antibody against CLIC4, the serum was first passed through a column containing purified CLIC5. The cross-adsorbed serum was then affinity purified using the AminoLink® Plus Immobilization Kit (Thermo Scientific).

Cell culture, infections and transfections

Human HeLa and MDA-MB-231 cells were grown in Dulbecco's modified Eagle's medium (DMEM) supplemented with 10% fetal bovine serum (FBS) at 37℃ under 5% CO_2. For CLIC4 and Rab35 knockdown studies, five distinct human CLIC4 (TRC human shRNA library; Sigma TRCN0000044358-TRCN0000044362) and two human Rab35 (TRC human shRNA library v2.0; Sigma TRCN0000380003 and TRCN0000380335) shRNAs in the lentiviral vectors pLKO.1 and pLKO TRC005, respectively, were used. Empty vectors were used as controls. To generate lentiviral particles for stable infection, HEK293T cells were transfected with the single RNA hairpins using the calcium phosphate protocol, and the virus was collected 48 h after transfection. CLIC4 and Rab35 stable knockdown and control cells were selected and maintained in medium with 2 μg/ml puromycin. Plasmid transfections for imaging studies were performed with X-tremeGene 9 (Roche) or Lipofectamine® (Invitrogen) reagents according to the manufacturer's instructions. Cells were lysed in JS buffer (50 mM HEPES pH 7.5, 150 mM NaCl, 1% glycerol, 0.5% Triton X-100, 1.5 mM $MgCl_2$, 5 mM EGTA, 20 mM Na-pyrophosphate, 10 mM Na_3VO_4) supplemented with protease inhibitor cocktail.

Cell adhesion and motility assays

For cell adhesion assays, cells were trypsinized and washed three times with DMEM supplemented with 0.1% BSA. 10^5 cells were seeded into 96-well plates coated with 1.5 μg/ml collagen type-I, 1.5 μg/ml fibronectin or no coating, and blocked with blocking buffer (DMEM plus 0.5% BSA). Cells were incubated for 30 min at 37℃ and non-adherent cells were removed by five washes using washing buffer (DMEM plus 0.1% BSA). Attached cells were fixed with 4% paraformaldehyde (PFA) for 10 min, washed twice and stained with Crystal Violet (5 mg/ml in 2% ethanol) for 10 min. Fixed cells were extensively washed with water and lysed with 2% SDS for 30 min. Plates were read at 490 nm.

To quantify cell spreading, focal adhesion size and focal adhesion number, cells were plated on collagen- or fibronectin-coated coverslips for 60 min as described above. Cells were stained with for F-actin with phalloidin (Cytoskeleton, Inc.) and anti-vinculin antibody and analyzed using ImageJ software as described (Margadant et al., 2012).

To measure random cell motility, cells were seeded on collagen-coated six-well plates, serum starved overnight and either stimulated with 1 μM LPA or left untreated. Phase-contrast images were acquired with a Zeiss Axiovert 200 M microscope equipped with a heated (37℃) chamber and CO_2 (5%) controller. Images were taken every 2 min during 8 h and the distance covered by the cells and cell directionality were analyzed using ImageJ software.

Fluorescence microscopy and image analysis

For imaging, cells were grown on collagen-I- or fibronectin-coated coverslips and fixed with 4% PFA for 10 min at room temperature. Fixed cells were permeabilized with 0.1% Triton X-100, 0.2% BSA in PBS for 10 min and subsequently blocked with 2% BSA in PBS, for 30 min at room temperature. Coverslips were incubated for 1 h with the indicated primary antibody, washed twice with PBS, and then incubated for 30 min with the Alexa-Fluor-conjugated secondary antibodies. Cells were washed twice with PBS and incubated for 5 min with DAPI prior to mounting with Immu-Mount™ (Thermo Scientific). Slides were examined on a Leica TCS-SP5 confocal microscope (63×objective).

For super-resolution microscopy using the ground-state depletion imaging method (Fölling et al., 2008), cells were cultured on 24 mm, no. 1.5 coverslips. After 24 h, cells were serum starved overnight prior to stimulation with LPA. Cells were washed briefly with PBS, fixed with 4% PFA for 10 min at room temperature and permeabilized with 0.1%

Journal of Cell Science (2014) 127, 5189–5203 doi:10.1242/jcs.150623

Triton X-100. Samples were extensively washed with PBS and blocked with 5% BSA for 30 min at room temperature. Coverslips were incubated for 1 h with the indicated primary antibodies at room temperature, washed and incubated with Alexa-Fluor-conjugated secondary antibodies (Alexa Fluor 647 and 532). Cells were imaged in the presence of an oxygen-scavenging system (10% glucose, 0.5 mg/ml glucose oxydase, 40 µg/ml catalase, 50 nM monoethanolamine). Imaging of the samples was carried out on a Leica SR-GSD microscope equipped with a 100× oil immersion objective (NA 1.47), using an additional tube magnification of 1.6×. Images were acquired in total internal reflection fluorescence mode at 100 frames per second, using an EM-CCD camera. Colors were sequentially imaged in decreasing wavelength order. Laser excitation wavelengths were 532 nm and 632 nm, using a QUAD filter cube.

Electron microscopy

For electron micrscopy studies, cells were fixed in 2% PFA plus 0.2% glutaraldehyde in 0.1 M PHEM buffer (60 mM PIPES, 25 mM HEPES pH 6.9, 2 mM MgCl2, 10 mM EGTA,) and then processed for ultrathin cryo-sectioning as described previously (Calafat et al., 1997). Briefly, 50-nm cryosections were cut at −120℃ using diamond knives in a cryo-ultramicrotome (Leica Aktiengesellschaft, Vienna, Austria) and transferred with a mixture of sucrose and methylcellulose onto formvar-coated copper grids. The grids were placed on 35-mm dishes containing 2% gelatin. Ultrathin frozen sections were incubated at room temperature with mouse monoclonal anti-β1 integrin antibody (TS2/16) followed by a rabbit anti-mouse bridging antibody and then incubated with 5-nm protein-A-conjugated colloidal gold (EM Lab, Utrecht University, The Netherlands) as a first marker. To block protein-A-binding sites, the sections were fixed for 10 min with 1% glutaraldehyde. Sections were then incubated with rabbit polyclonal anti-CLIC4 antibody, which was marked by 15-nm protein-A-conjugated colloidal gold. Immuno-labeled sections were embedded in a mixture of methylcellulose and uranyl acetate and examined with a Philips CM10 electron microscope (FEI Company, Eindhoven, The Netherlands).

Flow cytometry

For β1 integrin and EGFR surface expression analysis, cells were seeded in plastic dishes in complete medium with 10% FBS. At 24 h after plating, cells were trypsinized and washed three times with cold PBS supplemented with 1% BSA (washing buffer). 10^6 cells were incubated with anti-β1 (TS2/16) or EGFR (Ab-1) antibody in washing buffer for 30 min on ice, washed twice, incubated with secondary antibody (FITC-conjugated anti-mouse-IgG antibody, Rockland) for 30 min and washed twice again. Fluorescence measurements and data analysis were performed using BD FACSCalibur and CD CellQuest Pro software, respectively.

Integrin internalization and recycling assays

Confocal microscopy

To visualize integrin trafficking by confocal microscopy, cells were grown on collagen-I-coated coverslips and serum starved overnight. Anti-β1 integrin antibody TS2/16 was incubated with the cells at 4℃ for 1 h for surface integrin labeling. Antibody excess was removed by two washes with cold medium. Integrin internalization was allowed by incubation in serum-free DMEM for 2 h at 37℃. Recycling was induced by adding 10% FBS for 5 and 15 min. Cells were then fixed and processed for confocal analysis as described above.

Biochemical assays

Biochemical assays of integrin internalization and recycling were performed essentially as described earlier (Roberts et al., 2001). Briefly, cells were serum starved for 1 h and then washed twice with ice-cold PBS. Cell surface proteins were labelled using NHS-SS-Biotin (0.13 mg/ml) in PBS for 30 min at 4℃, and washed twice. For integrin internalization, cells were exposed to serum-free medium at 37℃ for the indicated time periods (0–15 min). Cells were transferred to ice and washed with cold PBS. Remaining biotin at the plasma membrane was reduced with sodium 2-mercaptoethane sulfonate (MesNa), and the reaction was quenched with iodoacetamide (IAA) before cell lysis.

For integrin recycling assays, cells were labeled with biotin as above, and incubated in serum-free medium at 37℃ for 30 min to allow internalization of cell surface integrins. Cells were returned to ice and washed twice with ice-cold PBS, and biotin was reduced using MesNa. Recycling of the internal pool was induced by adding 10% FBS at 37℃ for the indicated time periods (0–30 min). Cells were then returned to ice, washed twice with cold PBS and biotin at the cell surface was reduced by MesNa. MesNa was quenched by IAA and the cells were lysed. Biotin-labeled α5β1 integrin was detected by capture ELISA, using MaxiSorp 96-well plates (Nunc Thermo Scientific) coated with 5 µg/ml of anti-α5 integrin antibody.

To determine integrin degradation, cells were labeled with biotin and incubated in medium with 10% FBS for up to 6 h, whereafter the cells were lysed and biotin-labelled integrin α5β1 was detected by ELISA as described above.

FACS-based assays

The β1 integrin recycling assay was performed as described previously (Allaire et al., 2013). Briefly, cells were serum staved in recycling buffer (DMEM supplemented with 20 mM HEPES pH 7.5 and 0.1% BSA) for 1 h and incubated with anti-β1-integrin antibody TS2/16 (1 µg per 10^6 cells), at 4℃ for 1 h. Cells were washed twice with ice-cold recycling buffer and shifted to 37℃ for 30 min (pulse). Cells were cooled on ice and anti-β1-integrin antibody at the plasma membrane was stripped with two acid and salt washes (50 mM glycine, 150 mM NaCl, pH 2.5). Cells were then incubated in recycling buffer supplemented with 10% FBS and FITC-conjugated anti-mouse-IgG antibody (1:500) at 37℃ for the indicated recycling time, washed twice with cold recycling buffer, scraped off the plates and analyzed by flow cytometry as described above.

EGFR recycling, internalization and degradation assays

EGFR recycling assays were performed as described previously (Sigismund et al., 2008). Cells were serum starved in recycling buffer (DMEM plus 20 mM HEPES pH 7.5 and 0.1% BSA) for 4 h and incubated with 20 ng/ml EGF at 4℃ for 1 h. Cells were washed twice with ice-cold recycling buffer and shifted to 37℃ for 15 min (pulse). Cells were cooled on ice and residual EGF at the plasma membrane was stripped off with a mild acid and salt wash (0.2 M acetic acid and 0.5 M NaCl, pH 4.5). Cells were returned to 37℃ for the indicated recycling time (0–20 min), washed twice with cold recycling buffer, trypsinized and fixed with 4% PFA on ice. EGFR at the plasma membrane was stained with anti-EGFR antibody (clone Ab-1), and processed for flow cytometry as described above. For EGFR internalization, cells were serum starved overnight in serum starvation medium and incubated with 100 ng/ml EGF at 4℃ for 1 h. Excess of EGF was washed out by two washes with cold starvation medium and cells shifted to 37℃ for the indicated time points (0–15 min). Cells were trypsinized and fixed with 4% PFA on ice and treated as above for flow cytometry analysis. For EGFR degradation, cells were serum starved overnight and either left untreated or stimulated with 100 ng/ml EGF for the indicated time periods (0–180 min). Total cell lysates were loaded on SDS-PAGE and EGFR levels determined by anti-EGFR (clone 1005) immunoblot analysis.

Rab35-GTP pulldown assays

To measure the cellular levels of Rab35-GTP, the selective trap GST–RBD35 (the RUN domain of mRUSC2 fused to GST) was used as described previously (Fukuda et al., 2011). Briefly, shControl and shCLIC4 HeLa cells were transfected with 2×Myc–Rab35 and serum starved overnight. At 24 h after transfection, cells were stimulated with 1 µM LPA for 2 min or left untreated. Glutathione–Sepharose beads (GE Healthcare) coupled to 30 µg purified GST–RBD35 were incubated with 500 µg total cell lysate for 30 min at 4℃. Beads were washed three times and GTP-Rab35 bound to the beads was analyzed by immunoblotting using anti-Rab35 antibody. Total cell lysates were loaded on SDS-PAGE and GTP-Rab35 levels detected by anti-Myc immunoblot analysis.

Statistical analysis

For determination of statistical significance, unpaired Student's *t*-tests were performed using GraphPad Prism6 software. The indicated significance values are compared to control conditions. Box plots show median and 25th and 75th percentiles. *P*-values are indicated as follows: $*P<0.05$, $**P<0.01$, $***P<0.001$, $****P<0.0001$.

Acknowledgements

We thank Mitsunori Fukuda (Tohoku University, Sendai, Japan) for providing the GST-RDB35 construct; Mark Berryman (Ohio University, Athens, OH, USA), Dene Littler, Metello Innocenti, Pablo Secades (NCI, Amsterdam) and Jim Norman (Beatson Institute, Glasgow, UK) for helpful discussions; Lennert Janssen (NCI, Amsterdam), Dietmar Vestweber (Max Planck Institute, Münster, Germany) and Marina Gluckhova (Institut Curie, Paris, Francis) for reagents; and the NKI Microscopy and Flow Cytometry facilities for technical support.

Competing interests

The authors declare no competing interests.

Author contributions

E.A. conceived the study, designed and performed the experiments and analyzed the data. D.L.-P. and K.J. designed and performed super-resolution microscopy experiments studies. H.J. performed electron microscopy experiments. C.M. and A.S. analyzed the data and supervised the study. W.H.M. supervised and coordinated the study. E.A., C.M., A.S. and W.H.M. wrote the manuscript.

Funding

This work was supported by the Dutch Cancer Society (K.W.F.) and the Dutch Technology Foundation STW, which is part of the Netherlands Organisation for Scientific Research (NWO).

Supplementary material

Supplementary material available online at
http://jcs.biologists.org/lookup/suppl/doi:10.1242/jcs.150623/-/DC1

References

Allaire, P. D., Marat, A. L., Dall'Armi, C., Di Paolo, G., McPherson, P. S. and Ritter, B. (2010). The Connecdenn DENN domain: a GEF for Rab35 mediating cargo-specific exit from early endosomes. *Mol. Cell* **37**, 370-382.

Allaire, P. D., Seyed Sadr, M., Chaineau, M., Seyed Sadr, E., Konefal, S., Fotouhi, M., Maret, D., Ritter, B., Del Maestro, R. F. and McPherson, P. S. (2013). Interplay between Rab35 and Arf6 controls cargo recycling to coordinate cell adhesion and migration. *J. Cell Sci.* **126**, 722-731.

Arjonen, A., Alanko, J., Veltel, S. and Ivaska, J. (2012). Distinct recycling of active and inactive β1 integrins. *Traffic* **13**, 610-625.

Berry, K. L. and Hobert, O. (2006). Mapping functional domains of chloride intracellular channel (CLIC) proteins in vivo. *J. Mol. Biol.* **359**, 1316-1333.

Berry, K. L., Bülow, H. E., Hall, D. H. and Hobert, O. (2003). A C. elegans CLIC-like protein required for intracellular tube formation and maintenance. *Science* **302**, 2134-2137.

Berryman, M. A. and Goldenring, J. R. (2003). CLIC4 is enriched at cell-cell junctions and colocalizes with AKAP350 at the centrosome and midbody of cultured mammalian cells. *Cell Motil. Cytoskeleton* **56**, 159-172.

Böttcher, R. T., Stremmel, C., Meves, A., Meyer, H., Widmaier, M., Tseng, H. Y. and Fässler, R. (2012). Sorting nexin 17 prevents lysosomal degradation of β1 integrins by binding to the β1-integrin tail. *Nat. Cell Biol.* **14**, 584-592.

Bridgewater, R. E., Norman, J. C. and Caswell, P. T. (2012). Integrin trafficking at a glance. *J. Cell Sci.* **125**, 3695-3701.

Calafat, J., Janssen, H., Stahle-Backdahl, M., Zuurbier, A. E., Knol, E. F. and Egesten, A. (1997). Human monocytes and neutrophils store transforming growth factor-alpha in a subpopulation of cytoplasmic granules. *Blood* **90**,1255-1266.

Caswell, P. T. and Norman, J. C. (2006). Integrin trafficking and the control of cell migration. *Traffic* **7**, 14-21.

Caswell, P. T., Chan, M., Lindsay, A. J., McCaffrey, M. W., Boettiger, D. and Norman, J. C. (2008). Rab-coupling protein coordinates recycling of alpha5beta1 integrin and EGFR1 to promote cell migration in 3D microenvironments. *J. Cell Biol.* **183**, 143-155.

Caswell, P. T., Vadrevu, S. and Norman, J. C. (2009). Integrins: masters and slaves of endocytic transport. *Nat. Rev. Mol. Cell Biol.* **10**, 843-853.

Chaineau, M., Ioannou, M. S. and McPherson, P. S. (2013). Rab35: GEFs, GAPs and effectors. *Traffic* **14**, 1109-1117.

Chesneau, L., Dambournet, D., Machicoane, M., Kouranti, I., Fukuda, M., Goud, B. and Echard, A. (2012). An ARF6/Rab35 GTPase cascade for endocytic recycling and successful cytokinesis. *Curr. Biol.* **22**, 147-153.

Chua, C. E., Lim, Y. S. and Tang, B. L. (2010). Rab35 – a vesicular traffic-regulating small GTPase with actin modulating roles. *FEBS Lett.* **584**, 1-6.

Chuang, J. Z., Milner, T. A., Zhu, M. and Sung, C. H. (1999). A 29 kDa intracellular chloride channel p64H1 is associated with large dense-core vesicles in rat hippocampal neurons. *J. Neurosci.* **19**, 2919-2928.

Chuang, J. Z., Chou, S. Y. and Sung, C. H. (2010). Chloride intracellular channel 4 is critical for the epithelial morphogenesis of RPE cells and retinal attachment. *Mol. Biol. Cell* **21**, 3017-3028.

Dozynkiewicz, M. A., Jamieson, N. B., Macpherson, I., Grindlay, J., van den Berghe, P. V., von Thun, A., Morton, J. P., Gourley, C., Timpson, P., Nixon, C. et al. (2012). Rab25 and CLIC3 collaborate to promote integrin recycling from late endosomes/lysosomes and drive cancer progression. *Dev. Cell* **22**, 131-145.

Dulhunty, A., Gage, P., Curtis, S., Chelvanayagam, G. and Board, P. (2001). The glutathione transferase structural family includes a nuclear chloride channel and a ryanodine receptor calcium release channel modulator. *J. Biol. Chem.* **276**, 3319-3323.

Eichholtz, T., Jalink, K., Fahrenfort, I. and Moolenaar, W. H. (1993). The bioactive phospholipid lysophosphatidic acid is released from activated platelets. *Biochem. J.* **291**, 677-680.

Fölling, J., Bossi, M., Bock, H., Medda, R., Wurm, C. A., Hein, B., Jakobs, S., Eggeling, C. and Hell, S. W. (2008). Fluorescence nanoscopy by ground-state depletion and single-molecule return. *Nat. Methods* **5**, 943-945.

Fukuda, M., Kobayashi, H., Ishibashi, K. and Ohbayashi, N. (2011). Genome-wide investigation of the Rab binding activity of RUN domains: development of a novel tool that specifically traps GTP-Rab35. *Cell Struct. Funct.* **36**, 155-170.

Gagnon, L. H., Longo-Guess, C. M., Berryman, M., Shin, J. B., Saylor, K. W., Yu, H., Gillespie, P. G. and Johnson, K. R. (2006). The chloride intracellular channel protein CLIC5 is expressed at high levels in hair cell stereocilia and is essential for normal inner ear function. *J. Neurosci.* **26**, 10188-10198.

Geiger, B. and Yamada, K. M. (2011). Molecular architecture and function of matrix adhesions. *Cold Spring Harb. Perspect. Biol.* **3**, a005033.

Harrop, S. J., DeMaere, M. Z., Fairlie, W. D., Reztsova, T., Valenzuela, S. M., Mazzanti, M., Tonini, R., Qiu, M. R., Jankova, L., Warton, K. et al. (2001). Crystal structure of a soluble form of the intracellular chloride ion channel CLIC1 (NCC27) at 1.4-A resolution. *J. Biol. Chem.* **276**, 44993-45000.

Jiang, L., Salao, K., Li, H., Rybicka, J. M., Yates, R. M., Luo, X. W., Shi, X. X., Kuffner, T., Tsai, V. W., Husaini, Y. et al. (2012). Intracellular chloride channel protein CLIC1 regulates macrophage function through modulation of phagosomal acidification. *J. Cell Sci.* **125**, 5479-5488.

Jiang, L., Phang, J. M., Yu, J., Harrop, S. J., Sokolova, A. V., Duff, A. P., Wilk, K. E., Alkhamici, H., Breit, S. N., Valenzuela, S. M. et al. (2014). CLIC proteins, ezrin, radixin, moesin and the coupling of membranes to the actin cytoskeleton: A smoking gun? *Biochim. Biophys. Acta*. **1838**, 643-657.

Kouranti, I., Sachse, M., Arouche, N., Goud, B. and Echard, A. (2006). Rab35 regulates an endocytic recycling pathway essential for the terminal steps of cytokinesis. *Curr. Biol.* **16**, 1719-1725.

Littler, D. R., Assaad, N. N., Harrop, S. J., Brown, L. J., Pankhurst, G. J., Luciani, P., Aguilar, M. I., Mazzanti, M., Berryman, M. A., Breit, S. N. et al. (2005). Crystal structure of the soluble form of the redox-regulated chloride ion channel protein CLIC4. *FEBS J.* **272**, 4996-5007.

Littler, D. R., Harrop, S. J., Goodchild, S. C., Phang, J. M., Mynott, A. V., Jiang, L., Valenzuela, S. M., Mazzanti, M., Brown, L. J., Breit, S. N. et al. (2010). The enigma of the CLIC proteins: Ion channels, redox proteins, enzymes, scaffolding proteins? *FEBS Lett.* **584**, 2093-2101.

Lobert, V. H., Brech, A., Pedersen, N. M., Wesche, J., Oppelt, A., Malerød, L. and Stenmark, H. (2010). Ubiquitination of alpha 5 beta 1 integrin controls fibroblast migration through lysosomal degradation of fibronectin-integrin complexes. *Dev. Cell* **19**, 148-159.

Margadant, C., Monsuur, H. N., Norman, J. C. and Sonnenberg, A. (2011). Mechanisms of integrin activation and trafficking. *Curr. Opin. Cell Biol.* **23**, 607-614.

Margadant, C., Kreft, M., de Groot, D. J., Norman, J. C. and Sonnenberg, A. (2012). Distinct roles of talin and kindlin in regulating integrin α5β1 function and trafficking. *Curr. Biol.* **22**, 1554-1563.

Margadant, C., Kreft, M., Zambruno, G. and Sonnenberg, A. (2013). Kindlin-1 regulates integrin dynamics and adhesion turnover. *PLoS ONE* **8**, e65341.

Moolenaar, W. H., van Meeteren, L. A. and Giepmans, B. N. (2004). The ins and outs of lysophosphatidic acid signaling. *BioEssays* **26**, 870-881.

Muller, P. A., Caswell, P. T., Doyle, B., Iwanicki, M. P., Tan, E. H., Karim, S., Lukashchuk, N., Gillespie, D. A., Ludwig, R. L., Gosselin, P. et al. (2009). Mutant p53 drives invasion by promoting integrin recycling. *Cell* **139**, 1327-1341.

Padmakumar, V. C., Speer, K., Pal-Ghosh, S., Masiuk, K. E., Ryscavage, A., Dengler, S. L., Hwang, S., Edwards, J. C., Coppola, V., Tessarollo, L. et al. (2012). Spontaneous skin erosions and reduced skin and corneal wound healing characterize CLIC4(NULL) mice. *Am. J. Pathol.* **181**, 74-84.

Parsons, J. T. (2003). Focal adhesion kinase: the first ten years. *J. Cell Sci.* **116**, 1409-1416.

Pellinen, T. and Ivaska, J. (2006). Integrin traffic. *J. Cell Sci.* **119**, 3723-3731.

Ponsioen, B., van Zeijl, L., Langeslag, M., Berryman, M., Littler, D., Jalink, K. and Moolenaar, W. H. (2009). Spatiotemporal regulation of chloride intracellular channel protein CLIC4 by RhoA. *Mol. Biol. Cell* **20**, 4664-4672.

Powelka, A. M., Sun, J., Li, J., Gao, M., Shaw, L. M., Sonnenberg, A. and Hsu, V. W. (2004). Stimulation-dependent recycling of integrin beta1 regulated by ARF6 and Rab11. *Traffic* **5**, 20-36.

Qiu, M. R., Jiang, L., Matthaei, K. I., Schoenwaelder, S. M., Kuffner, T., Mangin, P., Joseph, J. E., Low, J., Connor, D., Valenzuela, S. M. et al. (2010). Generation and characterization of mice with null mutation of the chloride intracellular channel 1 gene. *Genesis* **48**, 127-136.

Rainero, E. and Norman, J. C. (2013). Late endosomal and lysosomal trafficking during integrin-mediated cell migration and invasion: cell matrix receptors are trafficked through the late endosomal pathway in a way that dictates how cells migrate. *BioEssays* **35**, 523-532.

Roberts, M., Barry, S., Woods, A., van der Sluijs, P. and Norman, J. (2001). PDGF-regulated rab4-dependent recycling of alphavbeta3 integrin from early endosomes is necessary for cell adhesion and spreading. *Curr. Biol.* **11**, 1392-1402.

Shukla, A., Malik, M., Cataisson, C., Ho, Y., Friesen, T., Suh, K. S. and Yuspa, S. H. (2009). TGF-beta signalling is regulated by Schnurri-2-dependent nuclear translocation of CLIC4 and consequent stabilization of phospho-Smad2 and 3. *Nat. Cell Biol.* **11**, 777-784.

Sigismund, S., Argenzio, E., Tosoni, D., Cavallaro, E., Polo, S. and Di Fiore, P. P. (2008). Clathrin-mediated internalization is essential for sustained EGFR signaling but dispensable for degradation. *Dev. Cell* **15**, 209-219.

Stauber, T. and Jentsch, T. J. (2013). Chloride in vesicular trafficking and function. *Annu. Rev. Physiol.* **75**, 453-477.

Steinberg, F., Heesom, K. J., Bass, M. D. and Cullen, P. J. (2012). SNX17 protects integrins from degradation by sorting between lysosomal and recycling pathways. *J. Cell Biol.* **197**, 219-230.

Suginta, W., Karoulias, N., Aitken, A. and Ashley, R. H. (2001). Chloride intracellular channel protein CLIC4 (p64H1) binds directly to brain dynamin I in a complex containing actin, tubulin and 14-3-3 isoforms. *Biochem. J.* **359**, 55-64.

Suh, K. S., Mutoh, M., Mutoh, T., Li, L., Ryscavage, A., Crutchley, J. M., Dumont, R. A., Cheng, C. and Yuspa, S. H. (2007). CLIC4 mediates and is required for Ca2+-induced keratinocyte differentiation. *J. Cell Sci.* **120**, 2631-2640.

Ulmasov, B., Bruno, J., Gordon, N., Hartnett, M. E. and Edwards, J. C. (2009). Chloride intracellular channel protein-4 functions in angiogenesis by supporting acidification of vacuoles along the intracellular tubulogenic pathway. *Am. J. Pathol.* **174**, 1084-1096.

White, D. P., Caswell, P. T. and Norman, J. C. (2007). alpha v beta3 and alpha5beta1 integrin recycling pathways dictate downstream Rho kinase signaling to regulate persistent cell migration. *J. Cell Biol.* **177**, 515-525.

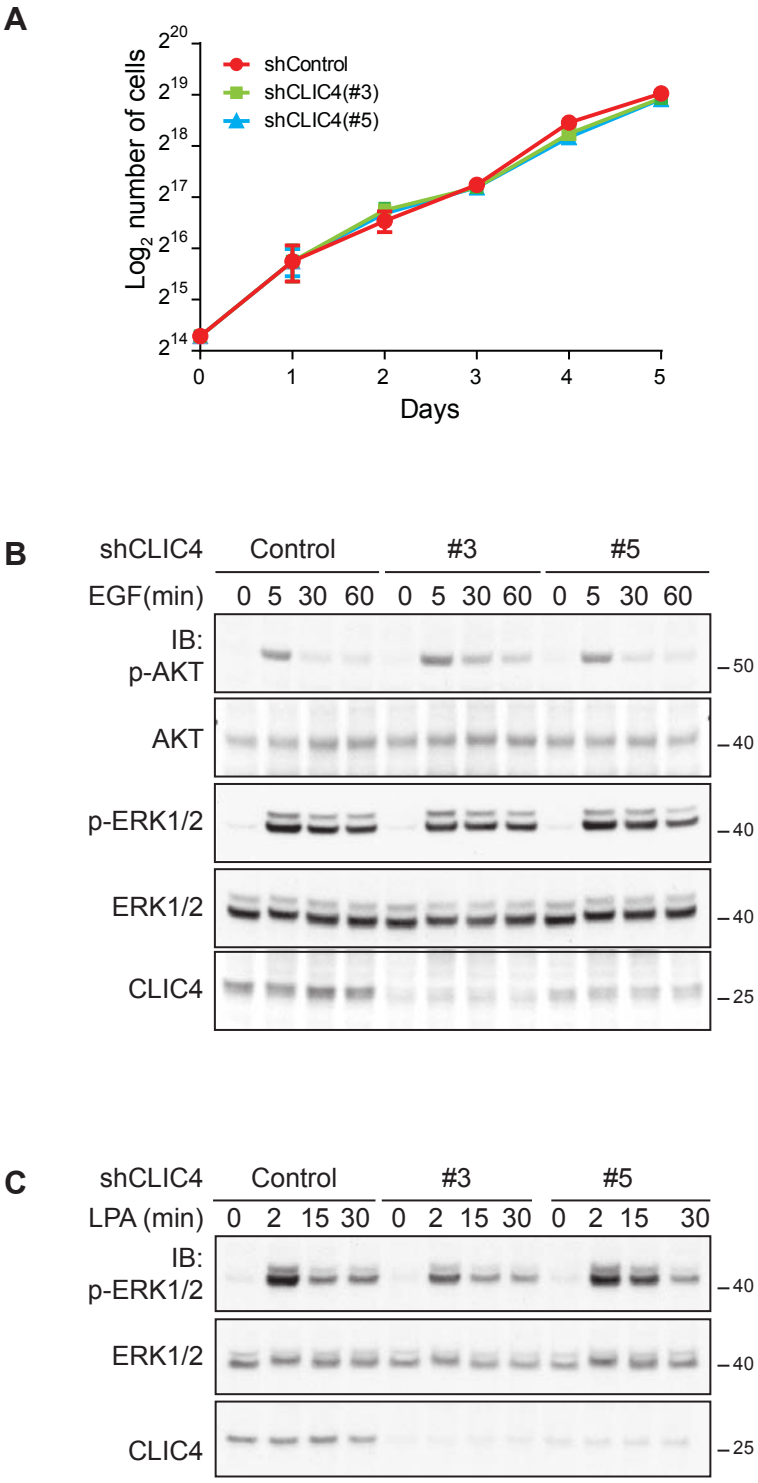

Figure S1. CLIC4 knockdown does not affect cell proliferation and growth factor signaling.
(A) Growth curves of shControl and shCLIC4 HeLa cells. (B-C) Growth factor-induced signaling. Serum starved shControl and shCLIC4 HeLa cells were left untreated or stimulated with 100 ng/ml EGF (B) or 5 μM LPA (C) for the indicated time points. AKT and ERK1/2 activation in time were monitored by immunoblot analysis of total cell lysates using anti-p-AKT and p-ERK1/2 antibodies. AKT and ERK were used as loading controls. Representative blots of one out of two experiments are shown.

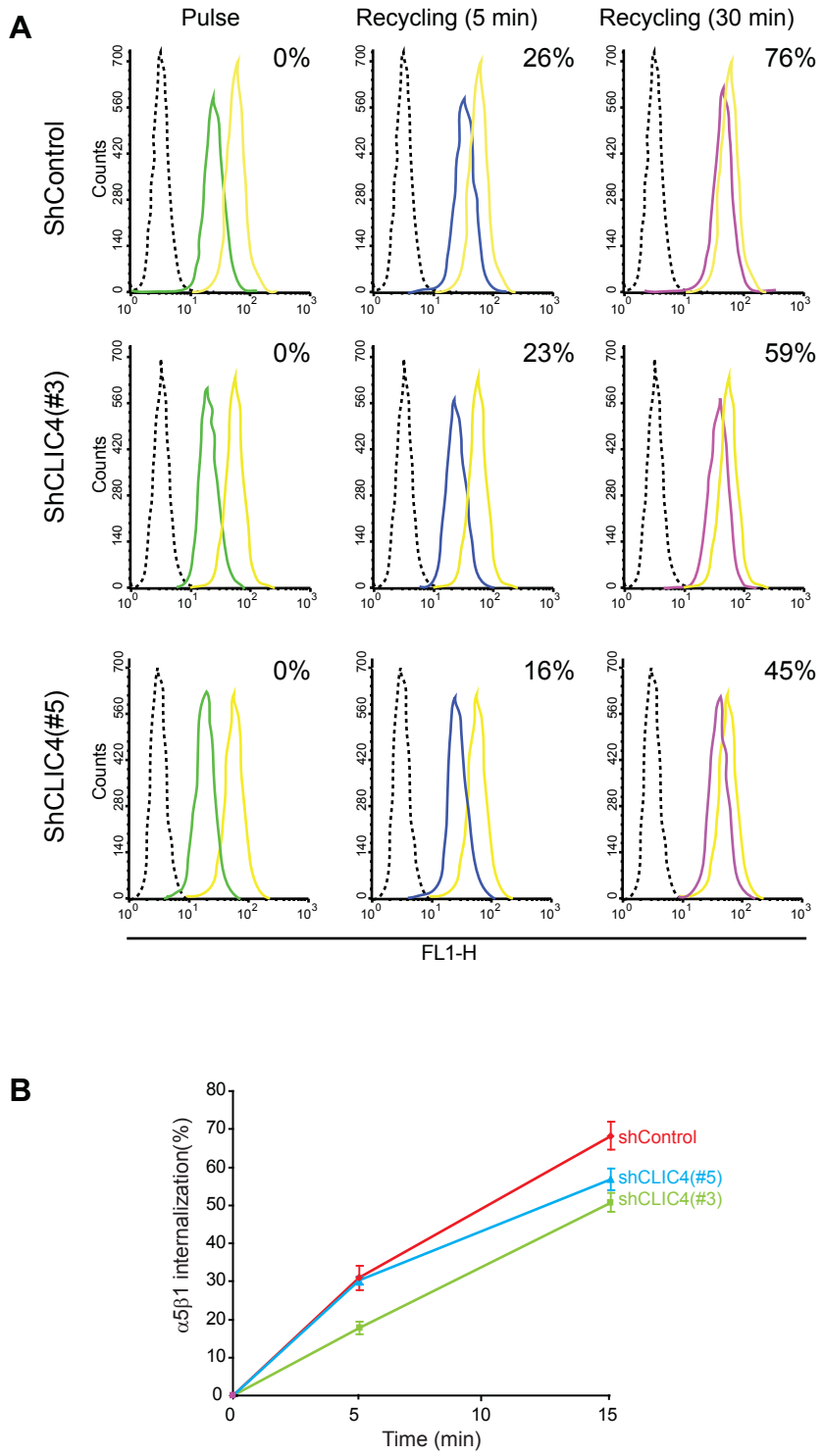

Figure S2. CLIC4 knockdown reduces recycling and internalization of α5β1 integrin

(A) FACS-based recycling assay. Serum starved shControl and shCLIC4 HeLa cells were incubated for 1 hour with anti-β1 antibody TS2/16 on ice. Cells were shifted at 37°C for 30 min (pulse), washed with an acidic buffer to strip the anti-β1 antibody at the plasma membrane and further incubated in presence of 10%FBS and FITC-conjugated secondary antibody for 5 and 30 min (recycling). Cells were gently scraped and analyzed by flow cytometry. Representative histograms of one out of two experiments are shown. Negative control= dashed black line, surface β1integrin = yellow line, Pulse= green line, 5 minutes recycling= blue line, 30 minutes recycling= magenta line. Percentage of recycled β1 integrin is shown. 50000 cells were analyzed for each time point.

(B) Biotin-based internalization assay. shContol and shCLIC4 HeLa cells were surface labeled with NHS-S-S-Biotin. Internalization was allowed to proceed for the indicated time points at 37°C. Cell surface biotin was reduced with MesNa at 4°C and the amount of internalized, biotin-labeled integrins was determined by capture ELISA using an anti-α5 integrin antibody. Data represent mean ± SEM of three independent experiments.

Table S1. CLIC4 knockdown does not affect expression of integrin α/β subunits.
Table showing expression of integrin α/β subunits. Cells were trypsinized, incubated with the indicated antibody against α- and β- integrin subunits and analyzed by flow cytometry. Staining with secondary antibody only was used as negative control. Geometric means ± SD from three independent experiments are shown.

	shControl		shCLIC4(#3)		
	Geo Mean	**SD**	**Geo Mean**	**SD**	**p-value**
FITC	3.69	0.57	3.12	0.44	0.059
alpha2	17.07	3.88	10.37	3.12	0.004
alpha3	38.84	13.77	36.20	11.79	0.856
alpha5	10.59	1.00	9.84	1.55	0.621
alpha6	30.53	7.93	29.51	12.77	0.932
alphav	23.17	1.96	18.09	0.26	0.068
beta1	45.23	9.10	39.95	11.85	0.407
beta3	3.93	0.67	3.20	0.57	0.058
beta4	8.67	1.53	7.30	1.44	0.456